Přírodovědecká fakulta
Faculty of Science

Jihočeská univerzita v Českých Budějovicích
University of South Bohemia in České Budějovice

Bachelor Thesis

Preparation of antibodies to determine the association of mitoribosomal complexes with mitochondrial membrane

Laura Zellner

Supervisor: Mgr. Ondřej Gahura, PhD
Laboratory of Molecular Biology of Protists
Institute of Parasitology, Biology Centre, Czech Academy of Sciences

České Budějovice, 2020

Zellner, L., 2020: Preparation of antibodies to determine the association of mitoribosomal complexes with mitochondrial membrane. Bc. Thesis, in English. – 57 p., Faculty of Science, University of South Bohemia, České Budějovice, Czech Republic

Annotation

The assembly pathways of mitoribosomes, descendants of bacterial ancestors producing proteins encoded by vestigial mitochondrial genomes, remains largely unknown. To shed light on structural features of a precursor of the highly divergent small mitoribosomal subunits (mtSSU) from *Trypanosoma brucei*, called mtSSU assemblosome, recently characterized by cryoEM, we raised antibodies against two assembly factors present in the complex and against two subunits of the mature mtSSU. We used the antibodies in pilot experiments to determine whether the assemblosome associates with the inner mitochondrial membrane.

I hereby declare that I have worked on my bachelor's thesis independently and used only the sources listed in the bibliography. I hereby declare that, in accordance with Article 47b of Act No. 111/1998 in the valid wording, I agree with the publication of my bachelor thesis, in full to be kept in the Faculty of Science archive, in electronic form in publicly accessible part of the STAG database operated by the University of South Bohemia in České Budějovice accessible through its web pages.

Further, I agree to the electronic publication of the comments of my supervisor and thesis opponents and the record of the proceedings and results of the thesis defence in accordance with aforementioned Act No. 111/1998. I also agree to the comparison of the text of my thesis with the Theses.cz thesis database operated by the National Registry of University Theses and a plagiarism detection system.

České Budějovice, …… …….

Laura Zellner

Acknowledgements

First and foremost, I would like to express my gratitude to my supervisor, Ondřej Gahura, without whom I would not have been able to complete this research project. Thank you for the enormous dedication and amount of time spent for patiently leading me through procedures, reviewing my writing and rekindling my enthusiasm when experiments did not provide the desired results. Moreover, I want to mention that I have learned a lot from his intellectual guidance.

Next, I would like to thank Alena for the great opportunity to become part of the lab and to improve my skills in molecular biology. I also wish to extend my special thanks to all of the members of the Lab of Functional Biology of Protists who very kindly welcomed and supported me.

Table of contents

Abbreviations

A	adenine
AA	amino acid
AAC	ADP/ATP carrier
ATP	adenosine triphosphate
BCA	bicinchoninic acid assay
bp	base pairs
BSA	bovine serum albumin.
DDM	n-Dodecyl β-D-maltoside
DNA	deoxyribonucleic acid
DTT	dithiothreitol
dNTP	deoxyribose nucleoside triphosphate
EDTA	ethylenediaminetetraacetic acid
EM	electron microscopy
EtOH	ethanol
FPLC	fast protein liquid chromatography
gDNA	genomic DNA
gRNA	guide RNA
6xHis	hexahistidine
Hsp70	heat shock protein 70 kDa
IPTG	isopropyl β-D-1 -thiogalactopyranoside
kDNA	kinetoplast DNA
LB	lysogeny broth
LD	loading dye
LSU	large subunit
mRNA	messenger ribonucleic acid
mt	mitochondrial
OD_{600}	optical density at 600 nm
PAGE	polyacrylamide gel electrophoresis
PCR	polymerase chain reaction
PF	procyclic trypomastigote
PNK	polynucleotide kinase
PVDF	polyvinylidene fluoride
RNAi	RNA interference
rpm	revolutions per minute
rRNA	ribosomal ribonucleic acid
RT	room temperature
SCoAS	succinyl-coenzyme A synthetase
SDS	sodium dodecyl sulfate
SSU	small subunit
tRNA	transfer ribonucleic acid
U	uracil
UV	ultraviolet
WCL	whole cell lysate
XGal	5-bromo-4-chloro-3-indolyl-β -D-galactopyranoside

1 Introduction

1.1 Translation

The synthesis of proteins based on translation of messenger ribonucleic acids (mRNA) is a molecular mechanism fundamental for life and was therefore studied extensively. The nucleotide sequence of mature mRNAs is translated by ribosomes, catalytic complexes consisting of small and large subunits (SSU and LSU), each composed of ribosomal RNA molecules (rRNAs) and several proteins. In the decoding centre of the SSU, mRNA basepairs with transfer RNAs (tRNAs) charged with amino acids (AA) according to the genetic code. AAs are linked by peptide bonds in the peptidyl transferase centre of the LSU to create nascent polypeptide chains. The peptide bond formation is catalysed by rRNA elements. Therefore, ribosomes are ribozymes (ribonucleic acid enzymes). After being synthesized, polypeptide-chains are folded into a three-dimensional structure and bind cofactors, can be modified by enzymes, or assemble with other protein subunits to become biologically active. Translation in cytoplasm is now understood in detail, however, not all aspects can be extrapolated to translation in organelles of endosymbiotic origin.

1.2 Translation in mitochondria

In early eukaryotic development, mitochondria evolved from an α-proteobacterium in endosymbiotic relationship with a protoeukaryotic cell. While the mechanism of this symbiotic event is not known, mitochondria's capacity to generate adenosine triphosphate (ATP) through aerobic respiration lead to their retention in host cells (Roger et al., 2017). The transformation from the autonomous endosymbiont to a cellular organelle involved various evolutionary changes like incorporation of transporters/carriers into the inner membrane of the prokaryote (Cavalier-Smith, 2006), integration of an organellar division mechanism into the host's cell cycle (Leger et al., 2015), as well as co-coordination of biochemical pathways in both symbiose partners (Braymer & Lill, 2017).

Additionally, mitochondrial (mt) genome was reduced to a bare minimum through the loss of redundant genes, and the gene transfer of essential genes to the host's nucleus (McCutcheon & Moran, 2012). This reduction was only possible due to the evolution of a faithful mechanism for import of host-encoded proteins into mitochondria (Wiedemann & Pfanner, 2017).

Since not all genes could be relocated to the nucleus (Daley & Whelan, 2005), mitochondria possess their own functional protein synthesis apparatus based on a degenerate bacterial ribosome elaborated by nucleus-encoded protein factors. The next paragraphs will in particular focus on the translation mechanism that evolved in the organelle.

Despite the initial assumptions that mt translation is highly similar to that of bacteria, it has become clear that mitochondrial protein synthesis is characterized by a number of unusual features (Kuzmenko et al., 2013). Remarkably, the mitochondrial genetic code deviates from the standard genetic code, for example UGA, recognized as a stop codon by cytoplasmic ribosomes, leads to the incorporation of tryptophan in mitochondria (Barrell et al., 1979). Also, mitochondrial tRNAs exhibit compacter structure and recognize more codons hence leading to a reduced number of different tRNAs needed for translation (Helm et al., 2000). However, in many species not all tRNAs are synthesized in mitochondria and are therefore imported from cytoplasm (Hancock & Hajduk, 1990). Another uniqueness of translation in mitochondria is the absence of anti-Shine-Dalgarno sequences in mt-mRNAs (Yusupova et al., 2001), which leads to a diversity of eukaryotic lineage specific translation initiation systems that yet need to be understand. Finally, recent studies also have shown that mitochondrial translation is tightly coupled to maturation and processing of mRNA (Kehrein et al., 2015).

Although ribosomes are universal for translation in all organisms, the structure and compositions of mitochondrial ribosomes (mitoribosomes) diverged from their prokaryotic ancestors, adapting to the requirements of the organelle (Petrov et al., 2019). Recent biochemical and structural data revealed that mitoribosomes are protein-rich, of bigger size compared to their bacterial counterparts and markedly divergent between individual lineages (Waltz & Giegé, 2019). The supplementary proteins are species-specific and form an interaction network on the surface of the conserved catalytic rRNA core that is responsible for decoding (Bieri et al., 2018; Ramrath et al., 2018). Several of the mitoribosomal proteins are characterized by pentatricopeptide repeat secondary structures, that are intended to bind single-stranded RNAs and therefore stabilize mitoribosomal structure (Ramrath et al., 2018). The proteins are recruited from cytosol during biogenesis to enable folding of the catalytic rRNA assisted by special assembly factors (Davis & Williamson, 2017).

Since most of mt gene products are highly hydrophobic membrane proteins, translating mitoribosomes are often bound to the inner mt membrane, facilitating insertion of the nascent polypeptides into the phospholipid bilayer (Pfeffer et al., 2015).

1.3 Mitochondrial gene expression in *T. brucei*

An extreme example in divergence of the mitoribosome is found in *Trypanosoma brucei,* the flagellate parasite causing human and livestock African trypanosomiasis (sleeping sickness). The illness is transmitted by tsetse flies (*Glossina* ssp.) infected by either *T. brucei gambiense* (which causes the chronic and most prevalent form of the disease) or *T. brucei rhodesiense* (resulting in a virulent and less common variation). Both forms initially resemble a common cold, evolving into a late stage manifestation in the central nervous system, that is often accompanied by sleep disruption, confusion, and coma (P. G. Kennedy, 2013). If untreated, the disease is almost always fatal. However, over the last few years several advances have been made in this field, leading the World Health Organization (WHO) to aspiring the eradication of human sleeping sickness in near future (P. G. E. Kennedy & Rodgers, 2019). Livestock African trypanosomiasis is nonetheless a threat to local African economy, hence research on trypanosomatids is still of importance.

T. brucei belongs to the class of Kinetoplastea and carries, like other euglenozoans, a single mitochondrion. Its mitochondrial deoxyribonucleic acid (DNA) is concentrated in a region called the kinetoplast (hence kinetoplast DNA, kDNA), which defines the taxonomic group. kDNA is composed of two separate entities known as maxicircles and minicircles (Liu et al., 2005). Maxicircles (~23 kb long) are present in 30-50 identical copies and contain a set of protein-coding genes typical for mitochondria (Benne et al., 1983) as well as cryptogenes that need massive editing in the form of uracil (U) insertions or deletions to be translatable (Feagin et al., 1988). Thousands of distinct ~1 kb long minicircles contain up to three guide RNA (gRNA) genes, which provide essential templates for the editing of maxicircle transcripts mentioned before (Pollard et al., 1990).

The polycistronic transcripts of both kDNA classes are made by mt RNA polymerase (Grams et al., 2002) and first have to be endonucleolytically cleaved into precursors of individual mRNAs (Koslowsky & Yahampath, 1997). Subsequently some mt RNA species are extended by 20 – 25 nt short 3’ poly adenine (A) or U tails that are later elongated to 120 – 250 nt, marking the transcript ready for translation (Etheridge et al., 2008). As a next step, immature transcripts are edited by the already mentioned U-insertions/deletions. Based on sequence homology with so-called anchor domains of gRNAs, the latter anneal to the pre-edited mRNA and start editing in 3’ to 5’ direction at the first basepair mismatch. Dozens of Us are either inserted or deleted before the gRNA is released again and the mature transcript can be translated (Read et al., 2016). An overview of the mt gene expression and translation is given in Figure 1.

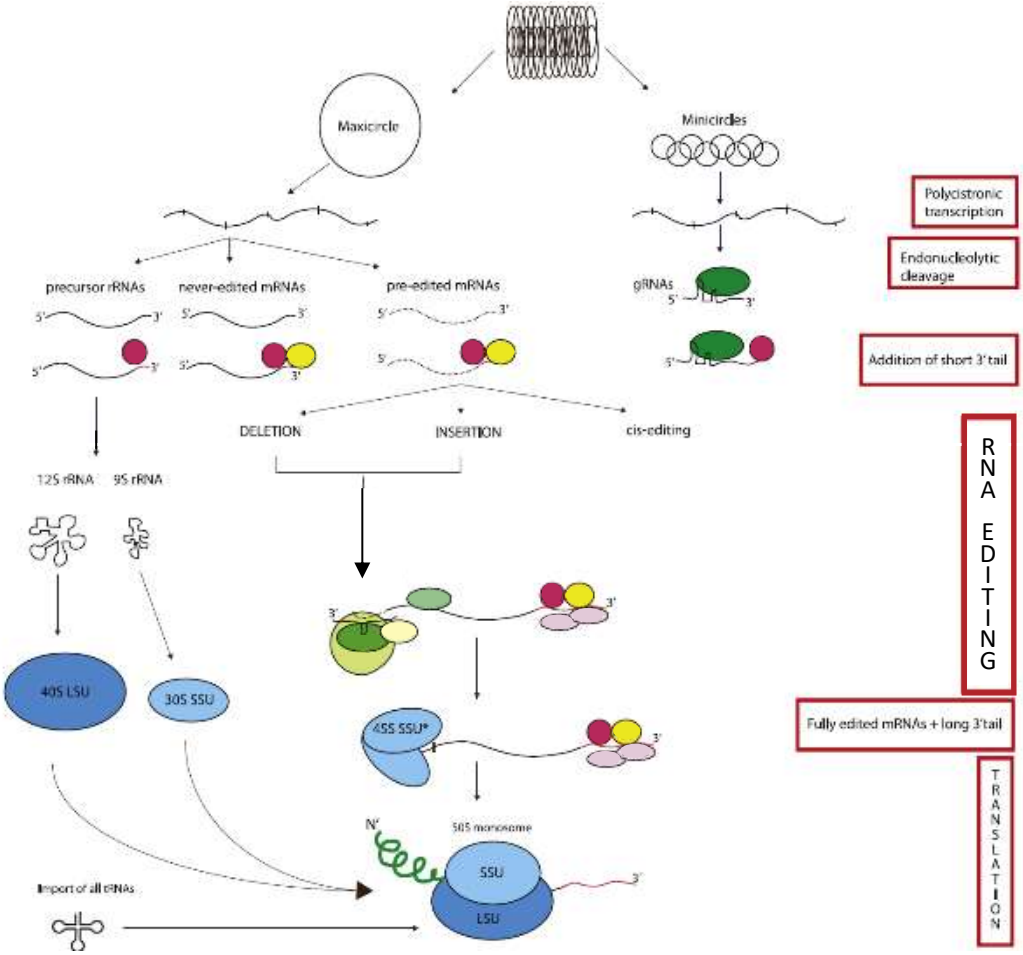

Figure 1: ***Gene expression in mitochondria of T. brucei****.*
From top to bottom: polycistronic transcription; endonucleolytic cleavage; adding of short 3' U tails. Several complexes assist in the maturation process.
(adapted from Verner et al., 2015)

1.4 Mitoribosomes of *T. brucei*

Mitoribosomes in *T. brucei* exhibit several unique properties not seen in other lineages. Their divergence is likely a consequence of adaptations to the atypical context of mt proteosynthesis in trypanosomatids (Niemann et al., 2011). Firstly, as mentioned above, translation is tightly linked to preceding RNA-editing. Secondly, the products of mt translation in trypanosomes are extremely hydrophobic. Thirdly, due to the absence of tRNAs from mt genome, nuclear-encoded tRNAs and their cognate AA-tRNA synthetases have to be imported with from the cytoplasmic pool (Lukes et al., 2005).

It is well established, that the fully assembled mitoribosome is protein-rich while carrying one of the smallest known rRNA molecules, which is encoded in kDNA maxicircles (Eperon et al., 1983). The small subunit (SSU) and large subunit (LSU) are only connected via 9 intersubunit bridges (Soufari et al., 2020), and mRNA channel, tRNA passage as well

as polypeptide exit tunnel are largely formed by trypanosomatid-specific proteins (Maslov et al., 2006; Scheinman et al., 1993; Sharma et al., 2003).

Recently the atomic structure of *T. brucei*'s mitoribosome was determined by cryo-electron microscopy (cryoEM) leading to more detailed understanding of the complex (Ramrath et al., 2018; Tobiasson et al., in press) (Figure 2).

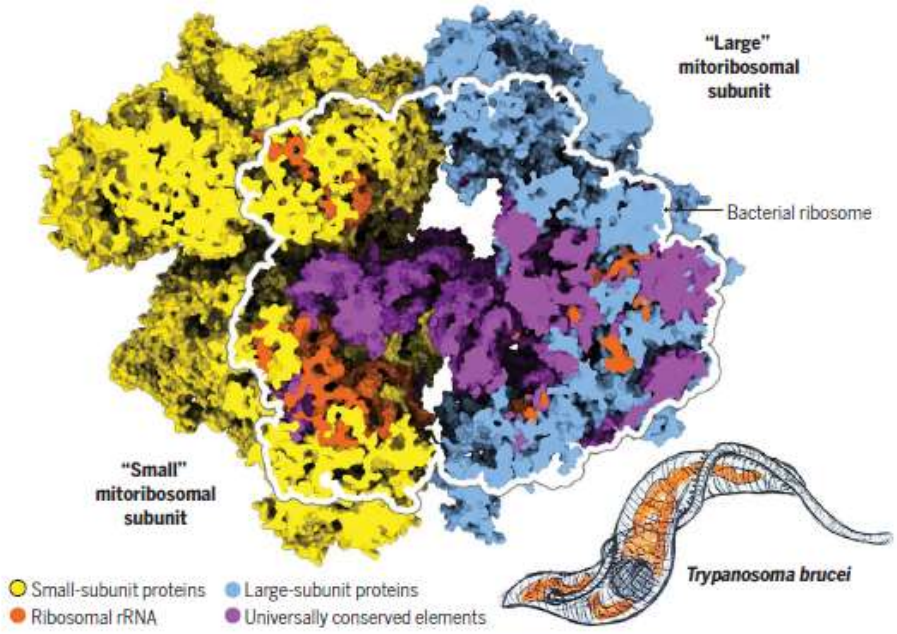

Figure 2: ***Trypanosomal mitoribosomes****. Cryo-EM reconstruction of the complete trypanosomal mitoribosome depicting the universally conserved core in comparison to bacterial ribosome. rRNA, which is extremely reduced in T. brucei, is to some extent substituted by additional proteins. (adopted from* Ramrath et al., 2018)

It was shown that the trypanosome mitoribosomes are larger than any other known ribosomes and show different overall morphology. The mtSSU contains 55 proteins, has a total mass of ~2.5 MDa, exceeding the size of bacterial SSU approximately three times, and it is larger than ~ 2 MDa mtLSU with its ~70 proteins. The protein scaffolds substitute the base-paired rRNA structure of other ribosomes. Outer shell proteins of mtSSU as well as mtLSU are lineage-specific while conserved regions are mostly found in the core (Ramrath et al., 2018). This attribute makes *T. brucei* an ideal organism for the identification of the minimal set of components required for functional ribosome activity.

Remarkable features of trypanosomal mitoribosome also include (1) that the SSU features a massive beak region considerably increasing its head's size, (2) a polypeptide tunnel with two exits and (3) the homology of some of its proteins to enzymes, repurposed for purely structural function (Ramrath et al., 2018). Due to the uniqueness of *T. brucei's* mitoribosome, the understanding of the machinery for mitoribosomal assembly is also of great interest.

Recently several precursors of trypanosomal mtLSU (Jaskolowski et al., 2020; Soufari et al., 2020; Tobiasson et al., in press) and mtSSU (Saurer et al., 2019) were identified.. Structure analysis of the earliest and largest assembly intermediate of mtSSU, the mtSSU assemblosome (Figure 3), enabled to identify several non-ribosomal assembly factors involved in the mtSSU biogenesis. The overall morphology of the assemblosome does considerably differ from mature mtSSU: With its 3.6 MDa and >70 proteins it is much bigger and more complex than any mitoribosome assembly intermediate described so far. It represents a mid-late stage of biogenesis lacking some components of the mature SSU and containing additional conserved or newly identified assembly factors. Indeed, a significant part of SSU rRNA in the assemblosome is in a premature conformation. Whereas its head is nearly completed, the rest of the complex requires massive reshaping and recruitment of additional proteins for maturation.

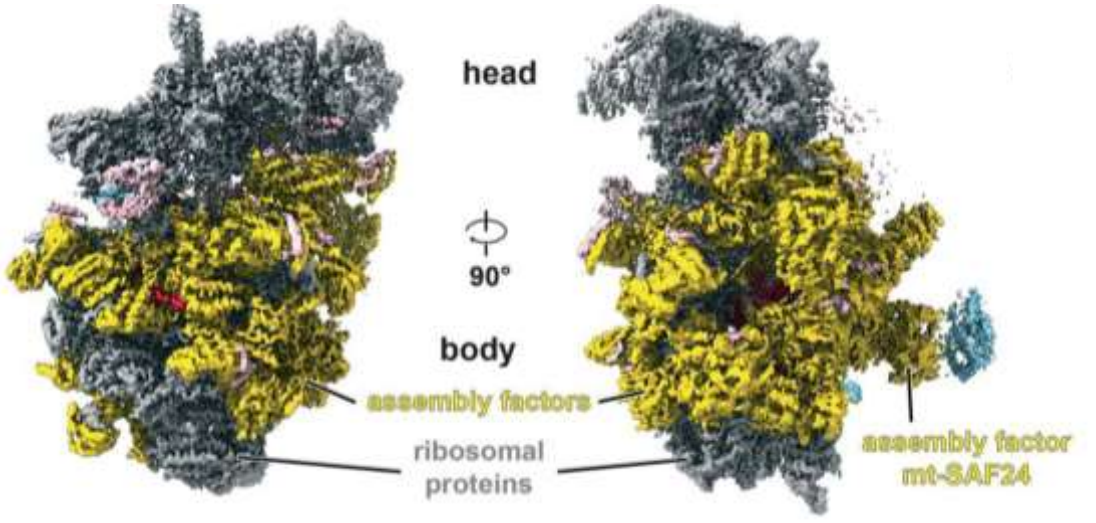

Figure 3: ***The structure of the trypanosomal mt-SSU assemblosome.***
Cryo-EM reconstruction showing ribosomal proteins (grey), assembly factors (yellow), rRNA (red), and unidentified proteins (pink).
Unidentified densities (light blue) on top of the assembly factor mt-SAF24.
(adapted from Saurer et al., 2019)

The biogenesis of mitoribosomes in general remains poorly understood. Only several assembly factors, most with prokaryotic homologs, have been described (De Silva et al., 2015). To achieve a first snapshot of the mitoribosome assembly pathway recently received structural data of the mtSSU assemblosome are further interpreted. One special feature of the assemblosome is a tower-like protrusion on its intersubunit side formed by a homopentameric assembly factor (mtSAF24; Figure 3 and 4; Saurer et al., 2019; Tobiasson et al., in press). Cryo-EM constructions show an unidentified part associated with this protein that might correspond to a phospholipid bilayer (Tobiasson et al., in press), which would indicate the linkage of mtSSU assembly to the inner mt membrane.

The recent structures of trypanosomal mitoribosomes and their assembly intermediates raised number of additional questions related to the function and biogenesis of the protein synthesis apparatus. Our goal is to address some of these questions by various biochemical techniques. In this project, antibodies against mtSSU components or assembly factors were raised to track the mitoribosome and its precursor. Specifically, assembly factors mtSAF24 and mtSAF18 and the two ribosomal proteins, bS6m and bS21m were chosen as targets. mtSAF24 forms the abovementioned assemblosome specific protrusion. mtSAF18 appears to be a homolog of a conserved assembly factor of bacterial and mitochondrial ribosomes, RbfA (our unpublished observation), localized in the core of the complex, stabilizing the so called central pseudoknot of mtSSU rRNA in its immature conformation. Further, mtSAF18 contributes to the recruitment of lineage specific assembly factors required for maturation of the decoding centre, where tRNA anticodons recognize mRNA. Whereas bS6m is already present in the mtSSU assemblosome, bS21m is recruited in later stages of biogenesis. The antibody against bS21m is therefore needed to distinguish mature mtSSU from the assemblosome in sedimentation experiments, because they do not differ sufficiently in size. Positions of all selected proteins in mtSSU and the assemblosome, as well as interaction partners of mtSAF18 are shown in Figure 4.

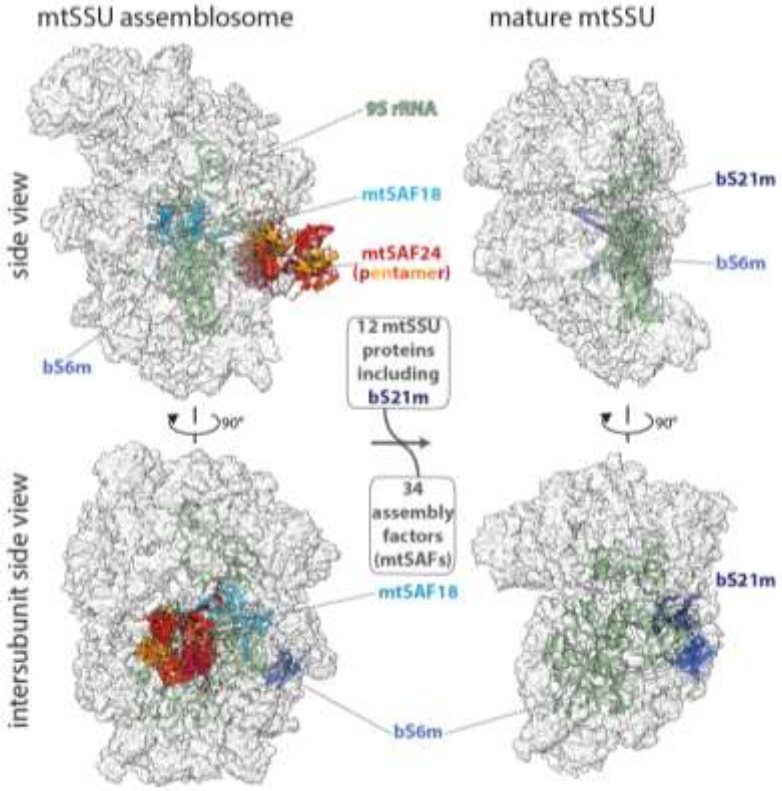

Figure 4: ***Models of mtSSU assemblosome and mtSSU.***
Proteins selected for antibody production are shown in cartoon representation and coloured individually. All other proteins are shown as semitransparent white surfaces. 9S rRNA is show as green ribbon.

2 Aims of the Thesis

- Prepare expression vectors for production of recombinant bS21m, bS6m, mtSAF18 and mtSAF24 and express and purify the proteins as antigens for antibody preparation
- Verify the new anti-bS21m, anti-bS6m, anti-mtSAF18 and anti-mtSAF24 antibodies on the recombinant proteins and trypanosomal whole cell lysates.
- Confirm mitochondrial localization of all targets by probing organellar and cytoplasmic fractions.
- Perform pilot experiments to determine the association of trypanosomal mitochondrial ribosomes and their assembly intermediates with the inner mitochondrial membrane

3 Methods

3.1 DNA techniques

3.1.1 Polymerase chain reaction.

Coding sequences of genes of interest were amplified from genomic DNA (gDNA) isolated from the wild type *T. brucei* procyclic strain (PF) 427 by polymerase chain reaction (PCR) with high fidelity KOD Hot Start DNA Polymerase (Novagen). To enable subsequent cloning of the PCR product into a vector, the restriction sites for *Nde*I and *Xho*I were included in the forward and reverse primer, respectively. Also three additional nucleotides were added to 5'ends of all primers to facilitate restriction digest. All primers are listed in Table 1. Reaction mixtures (Table 2) and cycling conditions (Table 3) were set according to the manufacturer's instructions and primers melting temperatures.

Table 1: PCR primers (restriction sites in bold; extensions for cloning in grey)

gene	forward primer	reverse primer
mtSAF18	ACT**CATATG**GTAAACAAGCAAACTCAG	ATA**CTCGAG**TTAGCGAACGAATTGAG
bS6m	ACT**CATATG**GTTTTTTATTCTTTTGTACTGGTGATG	ATA**CTCGAG**TCAGTTTCTCAGAAAACTGG
bS21m	ACT**CATATG**GGTGGTTACATGATGTAC	ATA**CTCGAG**TTAATTCACCCTCCAC

Table 2: PCR reaction mixture

reagent	[stock]	volume
gDNA	35 ng/µl	1 µl
buffer for KOD hot start DNA polymerase (Novagen)	10x	5 µl
$MgSO_4$	25 mM	3 µl
mixture of deoxyribose nucleoside triphosphates (dNTPs)	2.5 mM each	5 µl
forward primer	10 µM	5 µl
reverse primer	10 µM	5 µl
KOD hot start DNA polymerase (Novagen)		1 µl
MilliQ		25 µl

Table 3: PCR cycling conditions

step	temperature	time	cycles
polymerase activation	95°C	2 min	
denaturing	95°C	20 sec	3
annealing	50°C	10 sec	
extension	70°C	30 sec	
denaturing	95°C	20 sec	27
annealing	60°C	10 sec	
extension	70°C	30 sec	
elongation	70°C	2 min	

3.1.2 DNA gel electrophoresis.

PCR products and DNA fragments from restriction digestion were resolved on 1 % agarose gel in 1x TAE electrophoresis buffer (Table 4) with 1 µL of 10 mg/ml ethidium bromide per 70 ml of melted agarose. After the solidification of the gel, DNA samples with DNA loading dye (LD) (Table 5) added from 10x stock solution were loaded into the wells of the gel. For size reference 10 µl of GeneRuler 1kb Plus DNA ladder (Thermo Scientific, Figure 5) were loaded onto the gel. The electrophoresis was performed at 90 V for 40 to 60 minutes and the bands were visualized under ultraviolet (UV)-light using the ChemiDoc MP imaging system (Bio-Rad).

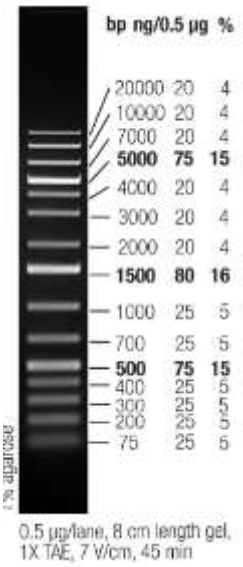

Figure 5: ***GeneRuler 1 kb plus DNA ladder*** *(adopted from Thermo Fisher Scientific - AT, n.d.)*

Table 4: 10x TAE buffer

reagent	[final]
tris	40 mM
acetic acid	200 mM
ethylenediaminetetraacetic acid (EDTA), pH 8.3	10 mM
MilliQ	

Table 5: DNA LD

reagent	[final]
glycerol	39 %
sodium dodecyl sulfate (SDS)	0.5 %
EDTA	10 mM
xylene cyanol	0.1 %
MilliQ	

Clean-up of PCR products

For purification of PCR products and removal of excess of primers, nucleotides, DNA polymerase and salts, GenElute PCR Clean-Up Kit (Sigma-Aldrich Co. LLC) was used according to the manufacturer's protocol. The kit is based on silica binding chromatography.

Concentration Measurement.

The yield and purity of PCR products and DNA fragments were determined by measuring absorbance at 260 nm (A_{260}) and A_{260}/A_{280} ratio, respectively, on a NanoDrop™ Spectrophotometer (Thermo Scientific).

3.1.3 Cloning into expression vector.

PCR products were inserted into the final protein expression vector pSKB3 via an intermediate cloning step into pGEM-T Easy (Promega).

Sub-Cloning into pGEM-T Easy.

To produce a 3´-deoxyadenosine overhang necessary for the subcloning step, 0.2 µl OneTaq® Polymerase and 7.5 µl OneTaq Standard Reaction Buffer (Biolabs Inc.) were added to each of the PCR products and samples were incubated at 72°C for 10 min. After a clean-up step (Gen Elute PCR Clean-Up Kit) ligation reactions were set and incubated for 1 hour at RT (room temperature) (Table 6).

Table 6: Ligation reaction mixture

reagent	**volume**
10x ligase buffer (Promega)	5 µl
pGEM-T Easy (Promega)	1 µl
T4 DNA ligase (Promega)	1 µl
PCR product	1 µl (50 – 100 ng)
MilliQ	2 µl

The products were transformed into competent *E. coli* cells strain XL1-Blue as described in section 7.2.3 and were plated onto lysogeny broth (LB) agar plates containing 100 µg/ml ampicillin, 1 mM isopropyl β-D-1-thiogalactopyranoside (IPTG; transcriptional inducer) and 40 µg/ml XGal. The pGEM-T Easy vector contains the lacZ gene coding for β-galactosidase fused in

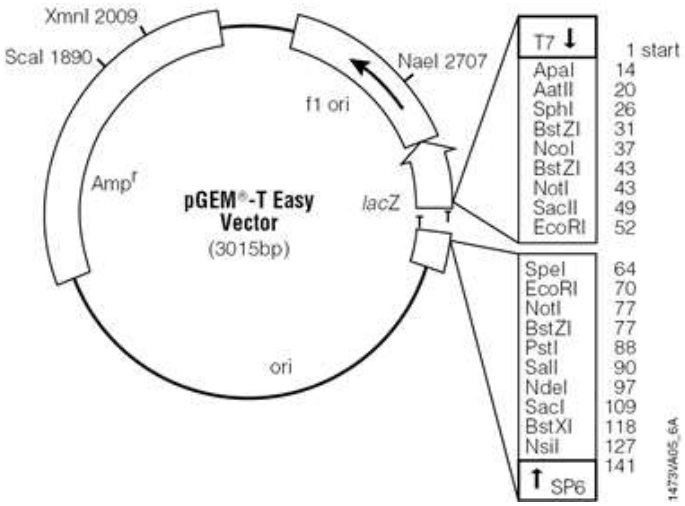

Figure 6: ***pGEM-T Easy (Promega) vector map****. The map shows antibiotic resistance, lacZ genes and available restriction sites. (adopted from Promega Corporation, 2018)*

frame with an α-peptide. Colonies with plasmid without inserts are blue, because XGal, a chromogenic substrate, is converted by the β-galactosidase into a blue product. If the α-peptide is interrupted by an insertion of a DNA fragment, the β-galactosidase is not produced, XGal is not hydrolysed, and the colony remains white.

Plasmids from white colonies were isolated from culture in liquid LB media containing ampicillin (1 µl/ml) grown at 37°C overnight using GenElute™ HP Plasmid Miniprep Kit (Sigma-Aldrich Co. LLC) according to manufacturer's protocol.

Restriction reactions were set according to Table 7 for 15 min at 37°C. For verification of the insert's correctness, DNA electrophoresis was performed as described above.

Table 7: Restriction reaction mixture

reagent	**volume**
FastDigest *Nde*I (ThermoFischer)	0.5 µl
FastDigest *Xho*I (ThermoFischer)	0.5 µl
10X FastDigest buffer (ThermoFischer)	2 µl
pGEM-T Easy + insert	3 µl (500 ng)
MilliQ	14 µl

Cloning into expression plasmid pSKB3 (Figure 7).

DNA fragments as well as pSKB3 vector backbone were prepared for cloning by gel extraction. For this purpose, an agarose gel was run, and the restricted DNA/vector fragments were isolated from the gel with the GenElute™ Gel Extraction Kit (Sigma-Aldrich Co. LLC). The DNA was then further purified by ethanol precipitation. Therefore, the samples were precipitated with 3M NaAc (⅒ of sample volume) and 96% Ethanol (EtOH) (2 sample volumes) and put to -80 °C for 10 min. DNA was pelleted at max speed for 10 min and the supernatants were removed. The pellets were incubated shortly at RT with 0.5 ml of 70% EtOH and spun again. Samples were dissolved in 20 µl MilliQ and concentration was measured.

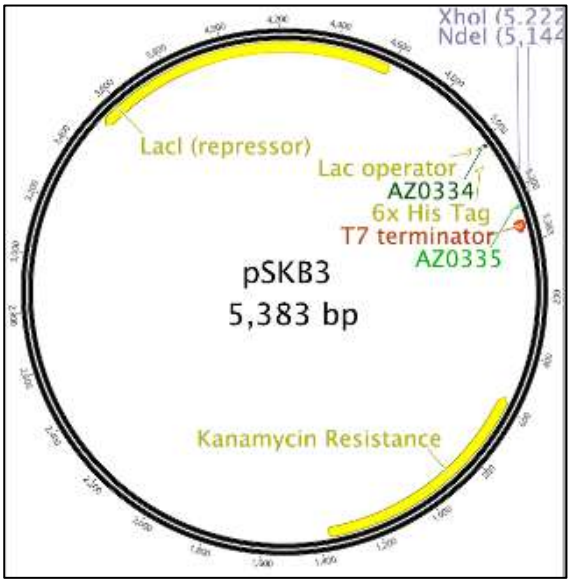

Figure 7: ***pSKB3 vector map****. including restriction sites XhoI and NdeI, antibiotic resistance and His-Tag. Primers AZ0334 and AZ0335 were used for verification of the inserts.*

Having prepared the linearized pSKB3 vector backbones as well as the recombinant sequences for the desired proteins, the ligation reaction was set overnight (Table 8). It was important to incubate the smaller amplicons with the larger vector backbone in a molar ratio of 3:1 to increase the probability of occurrence of the desired ligations.

Table 8: Ligation reaction mixture

reagent	**volume**
10x ligase buffer (Promega)	1.5 µl
pSKB 3 backbone (11.3 ng/µl)	4 µl (50 ng)
T4 DNA ligase (Promega)	1 µl
insert DNA	1 µl (15 – 20 ng)
MilliQ	3.5 µl

The ligation reactions were transformed into freshly prepared competent cells by electroporation (according to section 7.2.3) and plated onto kanamycin containing LB agar plates (section 7.2.2). The plates were incubated at 37°C overnight.

Verification of colonies by PCR.

Colonies were picked up from agar plates, DNA was amplified by PCR with OneTaq DNA Polymerase (Biolabs) using primers displayed in Table 9. Reaction mixture (Table 10) and cycling conditions (Table 11) were set according to manufacturer recommendation.

Table 9: PCR primers

	label	**sequence**
forward primer	AZ0334	ACAATTCCCCTCTAGAAA
reverse primer	AZ0335	CTTTCGGGCTTTGTTAG

Table 10: PCR reaction mixture

reagent	**[stock]**	**volume**
OneTaq standard reaction buffer (Biolabs)	5x	3 µl
dNTP's	10 mM	0.3 µl
forward primer	10 µM	1.5 µl
reverse primer	10 µM	1.5 µl
One*Taq* DNA polymerase (Biolabs)		0.075 µl
MilliQ		8.6 µl

Table 11: PCR cycling conditions

Step	**temperature**	**time**	**cycles**
initial denaturing	94°C	5 min	
denaturing	94°C	30 sec	30
annealing	50°C	30 sec	
extension	68°C	90 sec	
elongation	68°C	5 min	

3.2 Cultivation of *E. coli*

3.2.1 *E. coli* strains.

For plasmid construction and amplification *E. coli* strain XL1 Blue was used while recombinant proteins were expressed in the C41 strain.

3.2.2 LB broth and LB agar plates.

E. coli were grown in LB broth (Table 12) containing either 1 µl/ml ampicillin or kanamycin. Petri plates containing LB agar were made by addition of 7.5 g agar to 500 ml LB broth with lower salt concentration (171 mM NaCl). Antibiotics (100 µg/ml) were added to enable positive selection for bacteria containing the plasmid with resistance (ampicillin for pGEM-T Easy (Promega), kanamycin for pSKB3).

Table 12: LB broth

reagent	[final]
yeast extract	0.5 %
tryptone	1 %
NaCl	85 mM
MilliQ	

3.2.3 Transformation.

By heat shock.

DNA products were transformed into freshly prepared competent *E. coli* cells, that were prepared by Calcium chloride method. *E. coli* cells from a frozen glycerol stock were inoculated in 5 ml of LB media overnight. In the next morning, 1 ml of the culture was diluted to 50 ml with LB media and again allowed to grow at 37°C until they reached an optical density OD_{600}=0.4. Cells were harvested at 8.000 revolutions per minute (rpm) for 10 minutes at 4°C and subsequently resuspended in 20 ml of cold 0.1M $CaCl_2$. After 30 min incubation on ice, they were again spun, the supernatants were discarded and pellets were resuspended in 4 ml of cold 0.1 M $CaCl_2$.

For transformation 5 µl of ligation reactions were mixed with 50 µl of cells. After 5 minutes of incubation on ice, the cells were heat-shocked at 42°C for 45 seconds. The reactions were put back on ice for one minute before 200 µl of SOC medium (Table 13) were added. Subsequently, the cells were allowed to recover for 1 hour at 37°C in the shaker before they were plated onto LB agar plates containing the corresponding antibiotics.

Table 13: Super optimal broth (SOC) medium

reagent	[final]
yeast extract	0.5 %
tryptone	2 %
NaCl	10 mM
KCl	2.5 mM
$MgSO_4•7H_2O$	10 mM
$MgCl_2•6H_2O$	10 mM
glucose	20 mM
MilliQ	

By electroporation.

Transformation by electroporation was performed using the electroporator BTX ECM 630. This process relies on a brief, high-voltage electric field pulse that induces transient pores into the cell membranes, permitting the entry of the plasmids into the cells. 50 µl competent cells and 3 µl of ligation reaction were therefore mixed and put into a 0.2 cm cuvette. Cells were shocked using the following conditions: 2.5 kV, 200 Ω, and 25 µF. The time constant was 4 – 5 milliseconds. Immediately after the pulse 1 ml SOC medium (Table 13) was added, and the mixture was plated onto antibiotics containing LB agar plates.

3.3 Protein Techniques

3.3.1 SDS-PAGE.

For sodium dodecyl sulphate (SDS) polyacrylamide gel electrophoresis (PAGE) Tris-glycine 4-20 % Invitrogen Novex gradient gels (Thermo Fisher Scientific) were used. The electrophoresis chamber (Thermo Fisher Scientific) was filled with SDS-PAGE running buffer (Table 14) and the wells were rinsed by pipetting buffer. The samples and 4 µl unstained or prestained PageRuler Protein Ladder (Thermo Scientific; Figure 8) were loaded. The gels were run at 150 V for roughly 90 min or until the blue dye ran out of the gel's edge.

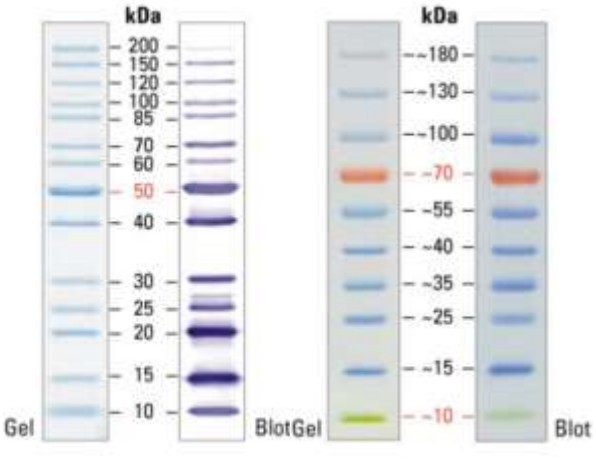

Figure 8: ***PageRuler protein ladders***
left: unstained for Coomassie staining
right: prestained for western blots
(adopted from Thermo Fisher Scientific - AT, n.d.)

Table 14: SDS-PAGE running buffer

reagent	[final]
SDS	0.1 %
glycine	192 mM
tris pH 6.8	25 mM
MilliQ	

Coomassie staining of SDS-PAGE gels

After electrophoresis, gels were rinsed with distilled water, submerged in Coomassie staining solution (Table 15) and gently shaken for 30 min. After removing of the stain and two quick washes with destaining solution (Table 16), the gels were left to destain in the destaining solution. The destaining solution was changed once after 30 minutes and a paper tower was added to accelerate the process. Destained gels were imaged on the Chemidoc.

Table 15: Coomassie staining solution

Reagent	[final]
methanol	50 %
Coomassie R-250	0.1 %
acetic acid	10 %
MilliQ	

Table 16: Destaining solution

Reagent	[final]
methanol	5 %
acetic acid	7 %
MilliQ	

3.3.2 Western blot and immunodetection with specific antibodies.

Proteins samples were transferred from the SDS-PAGE gels onto polyvinylidene fluoride (PVDF) membranes via electroblotting. For this reason, the gels were removed from the plastic cassettes while the membranes were charged by incubation in methanol for 40 sec. Gels, as well as membranes, were left to equilibrate in transfer buffer (Table 19) for at least 3 min. The blotting sandwich was prepared by layering cassette, pad, blotting paper, gel, membrane, blotting paper, pad, cassette and was subsequently placed into the transfer apparatus. The transfer was performed for 90 minutes at 90 V and 4°C.

After the transfer, the sandwich was disassembled, and the membranes were transferred to 50 ml conical tubes filled with 45 ml 5% skimmed milk in PBS-T (Table 18). The membranes were blocked rotating at RT for an hour to prevent unspecific antibody binding. Probing of the membranes was done by rotating the flasks overnight with specific primary antibodies diluted in 5 ml of 5% skimmed milk in PBS-T. Dilutions for individual antibodies are listed in Table 17.

Table 17: Primary antibodies; including size, localization in mt and affiliated secondary antibody

antibody	dilution	size	localization	secondary antibody (1:2000)
mtSAF18	1:500	42.2 kDa	to be tested	anti-rabbit
mtSAF24	1:250	12.2 kDa	to be tested	anti-rabbit
bS6m	1:250	18.8 kDa	to be tested	anti-rabbit
bS21m	1:250	23.0 kDa	to be tested	anti-rabbit
β	1:5000	71.5 kDa	membr. associated	anti-rabbit
AAC	1:2000	53.5 kDa	transmembrane	anti-rabbit
Hsp70	1:5000	34 kDa	mt matrix	anti-mouse
SCoAS	1:2000	44.9 kDa	matrix	anti-rabbit

Membranes were washed first for 5 minutes and then another three times for 5 to 10 minutes with 20 ml PBS-T. Washed membranes were probed rotating for 1 h with the goat or mouse anti-rabbit secondary antibody conjugated to horseradish peroxidase (Bio-Rad) diluted 1:2000 in 5 ml of 5% milk in PBS-T. Membranes were again washed in the same way as described above. To produce a chemiluminescent signal with the horseradish peroxidase, a Clarity Western ECL Substrate kit (Bio-Rad) was used. The peroxide reagent and the luminol/enhancer reagent were mixed in a 1:1 ratio and the membranes were exposed to the mixture for 60 sec. The chemiluminescent signal was visualized on the ChemiDoc instrument (Bio-Rad).

Table 18: PBS-T

reagent	[final]
10x PBS	1x
tween 20	0.05 %
MilliQ	

Table 19: Transfer buffer

reagent	[final]
tris	480 mM
glycine	390 mM
MilliQ	

Preparation of *T. brucei* whole cell lysates (WCL) samples for western blotting

WCL were prepared by spinning down $1x10^8$ cells at 1.300xg for 10 min at 12°C, decanting the supernatant and washing the pellet in 5ml PBS+G (Table 20) (1.300xg, 10min, 4°C). The sediment was resuspended in appropriate amount PBS plus 3x SDS LD, so that 30 µl of the WCL represented $1x10^7$ cells.

Table 20: PBS+G

reagent	[final]
10x PBS	1x
glucose	6 mM
MilliQ	

3.3.3 Expression test.

3 ml LB broth (section 7.2.2, Table 12) with kanamycin (1 µl/ml) were inoculated with *E. coli* strain C41 containing plasmids for expression of a recombinant protein and incubated in the 37°C shaker overnight. Next morning, the cultures were diluted to an optical density of OD_{600}=0.1 and again placed into the incubator. At a density of OD_{600}=0.4, 200 µl of the cells were harvested (10 000xg for 1 min), the supernatants were removed, and the pellets resuspended in 20 µl PBS (Table 21). 10 µl of 3x SDS-PAGE LD (Table 22) were added and samples were incubated at 96°C for 10 minutes to denature the proteins. The rest of the liquid cultures were induced by addition of IPTG to a final concentration of 1 mM. After three hours of growth another aliquot (induced) of 200 µl for each of the cultures was processed in the same way.

Table 21: PBS buffer

reagent	[final]
sodium phosphate, pH 8.0	20 mM
NaCl	500 mM
MilliQ	

Table 22: 3x SDS-PAGE LD

reagent	[final]
SDS	6 %
dithiothreitol (DTT)	300 mM
tris pH 6.8	150 mM
glycerol	30 %
bromophenol blue	0.02 %
MilliQ	

3.3.4 Solubility pilot assay with BugBuster.

To test the solubility and determine the strategy for purification of the recombinant proteins, a solubility assay with BugBuster was performed. Therefore 1 ml of induced culture was harvested by spinning at 4°C at 5000 rpm for 5 min. The pellets were flash-frozen in liquid nitrogen and then resuspended in 200 µl Bug Buster (RT) with 20 µl of 10x concentrated solution of protease inhibitors (Pierce) which was prepared by dissolving one tablet in water. After rotating the samples for 1 h at RT, they were spun at 16.000xg for 20 min at 4°C. The supernatants were transferred to new tubes and their volumes were measured. The insoluble pellets were resuspended in PBS (Table 21) using the same volumes as measured for the supernatants. 50 µl of each supernatant and resuspended insoluble fraction were mixed with 25 µl SDS LD respectively and incubated at 96°C in a heat block for 10 minutes.

3.3.5 Sarkosyl protein purification.

Expression of recombinant proteins in *E. coli*.

20 ml overnight cultures of *E. coli* C41 with respective expression plasmid were diluted to OD_{600} 0.1 in 500 ml of autoclaved LB media with kanamycin. At OD_{600} = 0.4 the cultures were induced with IPTG (1 mM) and left to grow in the 37°C shaker for three hours.

Sarkosyl Solubilization.

1 ml of each culture was harvested for WCL PAGE sample (as described above), pellets were resuspended in 100 µl PBS (Table 26) and 50 µl SDS LD. The remaining cultures were also pelleted by centrifugation at 8000xg for 10 min at 4°C, supernatants were discarded. After a wash in 25 ml of PBS (at 8000xg, 10 min, 4°C) the pellets were resuspended in 7.5 ml STE buffer (Table 25) with 2x protease inhibitors (Protease inhibitor tablets, Pierce). To receive a final concentration of 1 % Triton, additional 7.5 ml of STET buffer (Table 27) were added. Subsequently freshly prepared lysozyme solution (10 mg/ml, Table 23) was mixed to the resuspended cell pellets to achieve a final concentration of 10 mg/ml before they were incubated rotating for 30 min at 4°C. For removing nuclear DNA, $MgCl_2$ (30 mM) and DNase I (5 µg/ml, Table 24) were added and the samples were rotated at 4°C for another 10 min. Insoluble material was pelleted at 10.000xg at 4°C for 30 min, samples of 100 µl of the supernatants were kept for PAGE and mixed with 50 µl SDS LD.

Insoluble pellets were resuspended in 7.5 ml PBS, sarkosyl was added to a final concentration of 1.5 % and they were incubated overnight at 4°C. The next day the remaining insoluble material was removed by centrifugation (10.000xg, 30 min, 4°C) and the supernatants (soluble parts) were saved. Samples were taken from both the supernatant and the pellet, mixed with SDS LD and saved for PAGE analyzation (100 µl + 50 µl LD).

Lysates were filtered with a syringe filter (0.45 µm pores) and then were diluted to 15 ml with Buffer A (Table 28).

Table 23: Lysozyme

reagent	[final]
tris-HCl, pH 8.0	10 mM
lysozyme	10 mg/ml
MilliQ	

Table 24: DNase I (10 mg/ml)

reagent	[final]
tris-HCl, pH 7.5	10 mM
NaCl	50 mM
$MgCl_2$	10 mM
DTT	1 mM
glycerol	50 %
DNase I	10 mg/ml

Table 25: STE buffer

reagent	[final]
tris-HCl, pH 8.0	50 mM
NaCl	150 mM
EDTA	1 mM
MilliQ	

Table 26: PBS buffer, pH 7.4

reagent	[final]
sodium phosphate, pH 7.4	20 mM
NaCl	500 mM
MilliQ	

Table 27: STET buffer (2% triton)

reagent	[final]
tris-HCl, pH 8.0	50 mM
NaCl	150 mM
EDTA	1 mM
triton X-100	2 %
MilliQ	

Nickel affinity chromatography

Proteins were purified from lysates by nickel column affinity chromatography performed with the ÄKTAprime plus FPLC instrument (GE Healthcare). All buffers were filtered and degassed before starting the procedure. The ÄKTA was prepared by flushing the tubing with 20% ethanol to remove all air bubbles. Having flushed with ethanol, tube B was placed in a flask containing degassed milliQ water, the concentration of B was set to 100% with the inject valve position set to waste, and 25ml were allowed to run through the tube. Then tubing B was changed to a bottle containing buffer B (Table 30) and was filled with another 25 ml. After changing concentration of B to 0%, and inject valve position to load, ethanol was washed from the Ni-NTA column (5ml) by attaching the column to the ÄKTA, setting a flow rate of 5ml/min, and washing it through tubing A with MilliQ with another 50ml. Following the wash, tube A was filled with buffer A (Table 28), and the column was equilibrated with buffer A until UV280 stabilized (roughly 15 min). In the meantime, the fraction collector was filled with glass tubes and connected to the ÄKTA.

After preparation, the solution containing the protein was loaded through tubing A with a flow rate of 5 ml/min. Tube A was then changed to buffer A again and the machine was run until the lysate was loaded onto the column (UV reached a plateau). It was further washed with buffer A until UV traces stabilized again near the bottom of the graph, indicating that the flow-through is depleted of protein. Having established these conditions, it was proceeded to elution by setting a concentration gradient of 50 ml volume of buffer B reaching from 0 % to 100%. 2 ml fractions were collected and the UV absorption at 280 nm was monitored to observe peaks corresponding to eluted proteins. After the runs, the ÄKTA and the column were washed and stored in ethanol.

Table 28: Buffer A (Store at 4°C)

reagent	[final]
$NaPO_4$, pH 7.4	20 mM
NaCl	500 mM
imidazole	25 mM
sarkosyl	1 %
MilliQ	

Table 30: Buffer B (Store at 4°C)

reagent	[final]
$NaPO_4$, pH 7.4	20 mM
NaCl	500 mM
imidazole	500 mM
sarkosyl	1 %
MilliQ	

Table 29: 2.5M imidazole

reagent	[final]
imidazole	2.5 M
HCl / NaOH	pH 6.0
MilliQ	

Dialysis:

Purified proteins were dialysed in Membra-Cel dialysis tubings, MWCO 3000 (Serva). The membranes were sealed with clamps and placed in a beaker containing 500 ml dialysis buffer (Table 31) and a magnetic stirrer for 2 h at 4°C. The buffer was changed and left for another 2 h before the final dialysis step was set with 1 l of buffer overnight.

Table 31: Dialysis buffer

reagent	[final]
NaPO4, pH 7.4	20 mM
NaCl	250 mM
sarkosyl	0.8 %
MilliQ	

Protein concentration determination by bicinchoninic acid assay (BCA).

Protein concentration was determined by Pierce BCA Protein Assay Kit (Thermo Scientific) according to the manufacturer's protocol. Absorbance was measured at 562 nm and protein concentrations were calculated using a standard curve constructed by measuring a serial dilution of bovine serum albumin (BSA).

Proteins were further concentrated with protein concentrators Vivaspin 6, MWCO 3000 (Satorius) at 5.000xg.

3.3.6 Subcellular fractionation with digitonin.

For each subcellular fractionation $1x10^7$ procyclic *T. brucei* cells were harvested as described in section 7.3.2. Cells were kept on ice the whole time. After resuspending the pellet in 1.5 ml PBS+G (Table 20), the cells were spun at 1.300xg at 4°C for 10 min. The

supernatant was removed, and the cells were dissolved in 500 µl of SoTE (Table 32). The cells were lysed by addition of 500 µl of SoTE with 0.03% digitonin. The tube was inverted once prior to a 5 min incubation time on ice. Next, the sample was centrifuged at 7.000 rpm for 3 min at 4°C. The supernatant (cytosolic fraction) was transferred to a fresh tube and the volume was measured. The pellets (organellar fraction containing mitochondria) was resuspended in an equal supernatant volume of PBS. Both fractions were processed to SDS PAGE samples as described above.

Table 32: SoTE

reagent	**[final]**
tris-HCL, pH 7.5	20 mM
sorbitol	0.6 M
EDTA	2 mM
MilliQ	

3.3.7 Submitochondrial fractionation by sonication and carbonate extraction.

Mitochondria for further fractionation by sonication were isolated by hypotonic lysis. Therefore, $1x10^8$ *T. brucei* cells were harvested as described and washed in 1.5 ml of ice-cold NET (1.300xg, 10 min, 4°C) (Table 33). The cell pellet was resuspended in 1.5 ml of DTE (Table 34) and disrupted by passing through a 25G needle three times. Subsequently 180 µl of 60% sucrose were mixed to the lysates before spinning them again at 15.000xg (10min, 4°C). After aspiring the supernatants, the pellets were dissolved in 500 µl of STM (Table 35) and mixed with 1.5µl of 1M $MgCl_2$, 1.5µl of 0.1M $CaCl_2$ and 0.7µl of 10mg/ml DNase. Following 30 minutes incubation on ice, the DNase activity was stopped by addition of 500 µl of cold STE (Table 36). The solution was spun again, and the purified mitochondria were washed repeatedly with 500 µl of STE until the pellet was well formed and tough.

Table 33: NET

reagent	**[final]**
NaCl	150 mM
EDTA	100 mM
tris-HCl pH 8.0	10 mM
MilliQ	

Table 34: DTE

reagent	**[final]**
tris-HCl pH 8.0	1 mM
EDTA	1 mM
MilliQ	

Table 35: STM

reagent	**[final]**
sucrose	250 mM
tris pH 8.0	20 mM
$MgCl_2$	2 mM
MilliQ	

Table 36: STE

reagent	**[final]**
sucrose	250 mM
tris-HCl pH 8.0	20 mM
EDTA	10 mM
MilliQ	

Pellets containing mitochondria were dissolved in 500 µl of sonication buffer (Table 37), kept on ice the whole time and sonicated eight times for 15 sec at 30 % (ultrasonic homogenizer with a cup tip, model 3000 (BioLogics)). Between the individual sonication steps, the samples were allowed to cool down for roughly 10 sec on ice. Next, the cells were spun in a tabletop centrifuge at 10.000xg for 5 min at 4°C to remove any remaining intact mitochondria. The supernatants were transferred to open-top polyclear ultracentrifugation tubes and spun in SW40 Ti rotor (Beckman Coulter) at 24.000 rpm at 4°C overnight. Samples for western blots were prepared from supernatant (matrix fraction) and pellet (membrane fraction, including associated proteins) from one aliquot. The pellet was resuspended in 1 ml PBS + 500 µl SDS LD while the supernatant was mixed with 500 µl of SDS LD.

Table 37: Sonication Buffer

reagent	**[final]**	
sucrose	250 mM	
tris-HCL, pH 7.5	50 mM	
KCl	100 mM	
$MgCl_2$	10 mM	
DTT	3 mM	add fresh
EDTA	0.1 mM	
RNase inhibitors (Applied Biosystems)	400 u	add fresh
Pierce protease inhibitors (Thermo Fisher Scientific)	1 tablet / 50 ml	ass fresh
MilliQ		

Carbonate extraction was then applied to the pellets containing the mitochondrial membrane fraction in order to distinguish between integral membrane proteins and all other proteins associated with membrane by protein-protein or protein-lipid interactions. For this reason, the membrane fraction was resuspended in ice-cold 1 ml 0.1 M Na_2CO_3 and incubated on ice for 30 min. Before centrifugation in SW40 Ti rotor (Beckman Coulter) at 45.000 rpm for one hour (4°C), the samples were diluted to a total volume of 4 ml with 0.1 M Na_2CO_3 to avoid collapsing of the ultracentrifugation tubes. The pellets (integral membrane proteins) were again resuspended in an equal volume PBS as the supernatants (associated proteins) were measured. Both fractions were processed to SDS PAGE samples. All fractions from these procedures were analysed by SDS-PAGE and western blotting.

3.3.8 Analysis of mitoribosomes by fractionation on sucrose gradient.

Sucrose Gradient Fractionation of *T. brucei* lysates.

$1x10^8$ procyclic *T. brucei* cells were harvested by spinning at 1.300xg for 10 min at 4°C. Pellets were either snap-frozen in liquid nitrogen and stored at -80 °C for later use or processed

immediately. After a wash with SoTE buffer (Table 32), the cells were lysed in DM buffer (Table 39) with 400 units of RNase inhibitor (Applied Biosystems). The lysates were cleared by centrifugation at 17.000xg for 15 min at 4° and loaded on the top of 7-30% sucrose gradients in SGB buffer (Table 40) prepared with the Gradient Station (Biocomp) in open-top polyclear ultracentrifugation tubes for SW40 Ti Beckman rotor (Seton Scientific). The gradients were centrifuged at 50.000xg for 16 h in SW40 Ti rotor (Beckman Coulter). Subsequently 400 µl fractions of the gradients were collected with the Gradient Station connected to Triax UV cell.

Isolation of RNA from gradient fractions.

RNA was isolated by phenol-chloroform method by adding 200 µl phenol: chloroform: isoamyl alcohol (25:25:1 volume ratios) to 200 µl of every second fraction. After spinning at 12.000xg at 4°C for 15 min the upper aqueous phase was transferred into a new tube and mixed with 200 µl of chloroform. The fractions were spun again, the upper phase was recovered, and RNA was precipitated with 500 µl of isopropanol for 10 min at RT and pelleted (12.000xg, 4°C for 10 min). The pellet was washed with 500 µl 70 % ethanol at 12.000xg at 4°C for 5 min. The supernatant was discarded, and the pellet was dried on air for 5 min. After resuspension in 20 µl RNase-free water, RNA concentration was measured on NanoDropTM.

RNA Dot Blot, hybridization, and detection.

20 µl of RNA isolated from the gradient fractions were mixed with 40 µl of the sample buffer (Table 41), denatured by incubation at 65°C for 5 min, diluted by 60 µl of ice cold 20xSSC (Table 47), and incubated on ice for 3 min. 55 µl of each sample were transferred onto nylon membranes (Biodyne B, Pall Corporation) with 96-well Bio Dot microtitration apparatus (Bio-Rad) attached to a vacuum pump according to the manufacturer's instructions. RNA was immobilized by UV crosslinking with UV Stratalinker 1800 (Stratagene) in the autocrosslink mode. The membranes were incubated in prehybridization buffer (Table 43) at 42°C for 1 hour. Hybridization with ^{32}Phosphor(P)-labeled oligo probes (see below for labelling) was done overnight in hybridization buffer (Table 44). After three 30 min washing steps in 2x SSPE (Table 46) at 42°C, the membranes were exposed to a PhosphoImager screen for at least 24 hours and the exposed screen was scanned by a Typhoon Phosphoimager. The signal in individual dots was quantified in ImageQuant (GE Healtcare).

Oligo probe labelling.

Hybridization probes were prepared by phosphorylation of 5'termini of oligonucleotides (Table 38) with ^{32}P using T4 polynucleotide kinase (PNK; ThermoFisher Scientific). 50 pmol

of each oligo was mixed with 1 µl of 10x PNK buffer, 3 µl of γ-^{32}P-ATP (3000 Ci/mmol) and 1 µl T4 PNK in 10 µl reaction. The reactions were incubated at 37°C for 30 min and the excess of unincorporated γ-^{32}P-ATP was removed on a MicroSpin G25 column (GE Healtcare).

Table 38: Sequence of oligonucleotides used for hybridization

	sequence
9S rRNA (mtSSU)	ACGGCTGGCATCCATTTC
12S rRNA (mtLSU)	TGAACAATCAATCATGGTAATAAGTAGACGATG
18S rRNA (cytoplasmic SSU)	TGGTAAAGTTCCCCGTGTTGA

Table 39: 1x DM buffer

reagent	**[final]**	
tris-HCL, pH 7.5	50 mM	
KCl	100 mM	
$MgCl_2$	10 mM	
DTT	3 mM	add fresh
EDTA	0.1 mM	
DDM	1%	add fresh
MilliQ		

Table 40: 1x SGB buffer

reagent	**[final]**	
tris-HCL, pH 7.5	50 mM	
KCl	100 mM	
$MgCl_2$	10 mM	
DTT	3 mM	add fresh
EDTA	0.1 mM	
DDM	0.05%	add fresh
MilliQ		

Table 41: 1.5x sample buffer

reagent	**[final]**
MOPS buffer	1x
formamide	50%
formaldehyd	~ 6%
MilliQ	

Table 42: 100x dernhardt's solution

reagent	**[final]**
ficoll 400	2 %
polyvinylpyrrolidone	2 %
BSA	2 %
MilliQ	

Table 43: 1x prehybridization buffer

reagent	**[final]**
SSPE	6x
dernhardt's solution	5x
SDS	0.5%
herring sperm DNA	0.2 mg/ml
MilliQ	

Table 44: 1x hybridization buffer

reagent	**[final]**
SSPE	6x
dernhardt's solution	5x
SDS	0.1%
herring sperm DNA	0.02 mg/ml
MilliQ	

Table 45: 10x MOPS

reagent	**[final]**
MOPS	200 mM
$NaOAc•3H_2O$	50 mM
$EDTA•2Na•2H_2O$	10 mM
MilliQ	

Table 46: 20x SSPE

reagent	**[final]**
NaCl	3 M
$NaH_2PO_4x2H_2O$	230 mM
EDTA	25 mM
MilliQ	

Table 47: 20x SSC

reagent	**[final]**
NaCl	3 M
natriumcitrat	300 mM
MilliQ	

4 Results

4.1 Preparation of constructs for expression of recombinant mtSSU assembly factors and components

To produce antigens for antibody production, the coding sequences of mtSAF18, bS6m and bS21m, three specific proteins present in mtSSU or in the mtSSU assemblosome of *T. brucei*, were inserted into pSKB3, an expression vector, which was subsequently transformed into expression *E. coli* strain.

4.1.1 Amplification of coding sequences from genomic DNA by PCR.

Coding sequences were amplified by a proofreading polymerase to limit errors. Table 44 shows expected sequences of obtained products, including extensions from primers. Figure 9 shows the fragments after separation by electrophoresis on agarose gel. All fragments proved to have correct size and were at sufficient concentration for subsequent steps. Minor bands resulting from contamination can be observed, especially for mtSAF18, but they were negligible compared to the amount of correct product. Concentrations of PCR products are shown in Table 48.

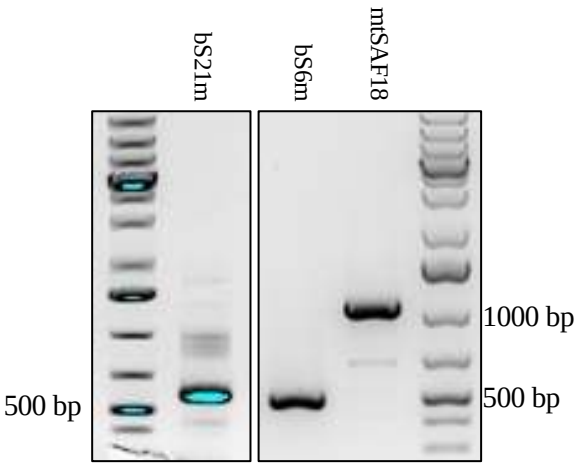

*Figure 9: **Amplicons of target genes on DNA gel**. The major bands represent fragments of bS21m, bS6m and mtSAF18 at the expected sizes of 573, 498 and 1080 nt, respectively. The sizes of some ladder bands are shown.*

Table 48: Sequences of PCR products containing coding sequences of the recombinant proteins (green: primers; blue: restriction sites; grey: non-specific nucleotides for cloning)

gene	length	PCR product
mtSAF18	1080 bp 42.4 kDa	ACTCATATGGTAAACAAGCAAACTCAGAAGTATCGTACGAAGTTACGCTACCGGTTCCGTCAACCG TCTGTTGTGCCGCTACGCCAAACCCTTCAGCAGCGCCACAACACGATCCTGGAAGTTCTGCGAAGA CGCAGGATAAACTCCGGCGATCAGTCTCCCTATCGATACGTGGAGGAACGACTATACTCTAAACCA TCGCGACTTGATCGTGAAGGTGTAAAGGTTAACAAAACGTACGCACTCAGGGCTTAGGTGATCTG GAGCCTCTCCGGTATGGTGCGAACTTTGGGATTTCTGAAAAGGATGCGTTAAAGTACGAAACCGT GGCCGAAAAAGCGAAGTACATGGAACCACCTATTCCCTACAGCTCCCTCGCGGCTCGGAAGCTAGC CGCTGGTGCGTTGTGGCCTGCTGCGCCAGACCCAGAAGGGATGATAAGCAAGGAGGTTCGACTAC TACGACATGAGTCAAGCATGTCCCCAAGCGCGCGTGCGTTTTCCGAAAGGGTAGCATACCACCTG CGGCGCTCGCTTAAAGCATGTCCAGGCCACATCGCTGAGCACATCGACTTTACGCAGCTTATCATAC AGGAGGTGTTGGGGTCCCGTCGCTCTAAAGAAATATATATTGTTTGGTTTACTGTAGATCCCGGGG CACGCTTTGAACTGGAGCCGCGTCTGCATCAGCTCAACCACTGGGTACAACAACTTATTATTAAGA GAGTGAAGCGCCGTCCTCATATCCCACGAGTGACATGGATTTATGATGGCGGAAGGCTTGAGCGT GAGCTACCACGTGATGTTAAGCAGGAATTGCAGAGTTTCGTGGCTGACGCAGCAACAACGCTGGA GAGTCGTGTAAAGTACTTAAAGGAACTTGACACAATGAATCAACGTATGAAGGATATACCGTGGT TTATGCCGTACTTGTGGAGCAAAGAGGAGAAGGCCGCGCGGCAGAAATCCATGCTAGCTGATCTT GAGGAGGTGGAGCGGAGGAAAAATGAACATAGTAGTGGACGAAGTGCACCGCCTCGCATGAGTC CTCCTCCTCAATTCGTTCGCTAACTCGAGTAT

bS6m	498 bp 18.8 kDa	ACTCATATGGTTTTTTATTCTTTTGTACTGGTGATGAAGCCACGACAACGTCGATTCACTTCGCAGG CGTTGCGTGAGATCGGTGTTGCTGTCTATAGCAACGGTGGTCTTATCAGAAGCATCACAAACGAGG GGATTATGCGGCCCTATAGTCGCTTCCGTGATGCAGACAATACGCCCTTAACGTATGCACGGTATA TTATACTTCAGCTTGACATGGGTGAGGAAGAAATGGGAAAGGTAGACAAAATCATACGGGAACAT CAGGACGTTTTGATGGCGCTAAAGTTGAACAACCTGGAGCGACCGGTGGGTATACGAAGTGGGAA TAAAGAACTACAGGCCGCTTACTTTCCGCTGGACACTTTCACGCGACTTGAGGAGGAAATTAACTG GTCACCTCAGACCTCAGCAGATATTTACACACAGTTGGAGATGAACTGGAAGGAATTCTCCCGCAC ACGTTGGTCCAGTTTTCTGAGAAACTGACTCGAGTAT
bS21m	573 bp 23.0 kDa	ACTCATATGGGTGGTTACATGATGTACCACCGCAAGGCGATGGGAACTATGAAGTACAGTAAGTG GAAGGGTGCTCACGGTGGTATCAGTCACTTCTACGGGCGCACGCCGATGGTTGAGGAAGTGCGGC CCAATGAGCCAATAACGCTGGTGGATCGACGTATCATGCATTACGTGCACCACTCACGGCTGCGTC ACTTTCAGTTGTTCCGCTCATATCAGGAAAAATCGAACTCAACGGAGTGCAAACTACGCGAGGGGG AGATGCTCCGGCGCCGCTGGCACCGGAGATTGCAAAAGTCGTTTATTGCATTCATGCAGTTCAAGA CAATGAAGGTCCTGGAGGATCAAGCGCGTCTGGTGAACACGTATGGGCAGGCAGCAGTGAATGC GGCACTTGGGGATCCTTGGAATGCAACAGATAATGTGGCCCGGGAGCGGAAGTCTGCGGCGGTCC GCCGGCAGGTGCGTGCACTCCCAATGGTTAATGTCGTACCAAAGCACGTTGCGACGATGAAGCAG ATTCATAACGATCGTTTCAACTATCGGTGGAGGGTGAATTAACTCGAGTAT

Table 49: Concentration of DNA products

PCR product	**volume** [µl]	**concentration** [ng/µl]
mtSAF18	20	32
bS6m	20	125
bS21m	20	85

4.1.2 Cloning into vector for expression of recombinant proteins.

PCR products were cloned into pGEM-T-Easy vector (Promega) by ligation using a 3´-deoxyadenosine overhang, followed by transformation into *E. coli* cells. Selected white colonies were grown in LB media, the bacteria were harvested, plasmid DNA was purified, and concentration was measured (Table 50).

Table 50: Concentration of plasmid DNA

clone	**volume** [µl]	**concentration** [ng/µl]
mtSAF18/1	75	173
mtSAF18/2	75	171
mtSAF18/3	75	170
mtSAF18/4	75	170
mtSAF18/5	75	181
bS6m/1	75	185.7
bS6m/2	75	182.5
bS6m/3	75	165.9
bS21m/1	75	155.7
bS21m/2	75	149.2
bS21m/3	75	143.6

Plasmids were digested with *Nde*I and *Xho*I and the results of the restriction analysis were visualized on agarose gels. Figure 10 shows/documents that plasmids bS21m/3, bS6m/2, bS6m/3 and all of inoculated colonies with mtSAF18, expect of mtSAF18/4, contained the correct insert. The band at roughly 3000 bp corresponds to the pGEM-T Easy (Promega)

backbone. The plasmids containing inserts of correct size for bS21m and bS6m as well as mtSAF18/1 and mtSAF18/5 were verified by Sanger sequencing.

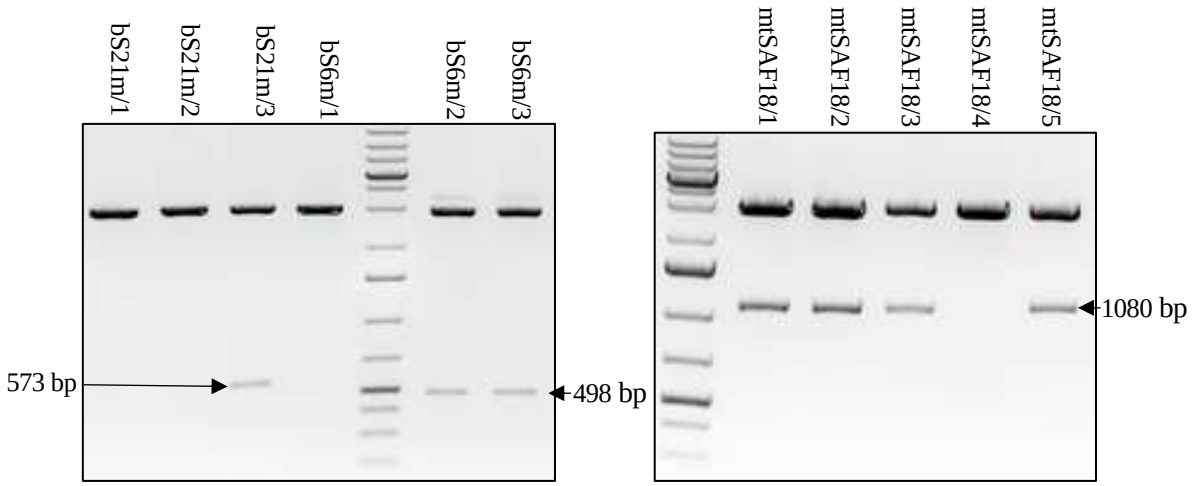

Figure 10: ***Restriction analysis of plasmids.***
Agarose gels visualizing digested clones containing bS21m / bS6m / mtSAF18 along with 1kb Plus DNA ladder. The band at ~3000 bp corresponds to the vector backbone.
Loading: 10 µl per restriction reaction + 1 µl LD

Cloning into expression vector pSKB3.

To enable purification of the recombinant proteins with nickel column affinity chromatography, the vector pSKB3 was chosen for their expression. The N-termini of the prepared protein coding sequences were ligated to the sequence for the hexahistidine (6xHis) tag in pSKB3 upstream from the cloning site (see Figure 7). A gene conferring resistance to kanamycin included in the vector was used for positive selection. The verified intermediate pGEM-T-Easy based plasmids and the vector pSKB3 were digested with *NdeI* and *XhoI*. The products were separated on agarose gels and the fragments as well as the pSKB3 vector backbone were purified by gel extraction. Next, the isolated DNA was precipitated by EtOH, dissolved in water and its yields were measured (Table 51).

Table 51: Concentration of excised DNA

fragment	**volume** [µl]	**concentration** [ng/µl]
mtSAF18	15	18.5
bS6m	15	8.9
bS21m	15	6
pSKB3	15	55

The DNA fragments were ligated into the vector and transformed by electroporation into *E. coli.* Three colonies from each ligation were analysed by colony PCR with primers specific for the respective inserts. Figure 11 shows that for each protein at least one bacterial colony contained the plasmid with an insert in the correct size. For expression, correct plasmids were transformed into C41 cells by heat shock.

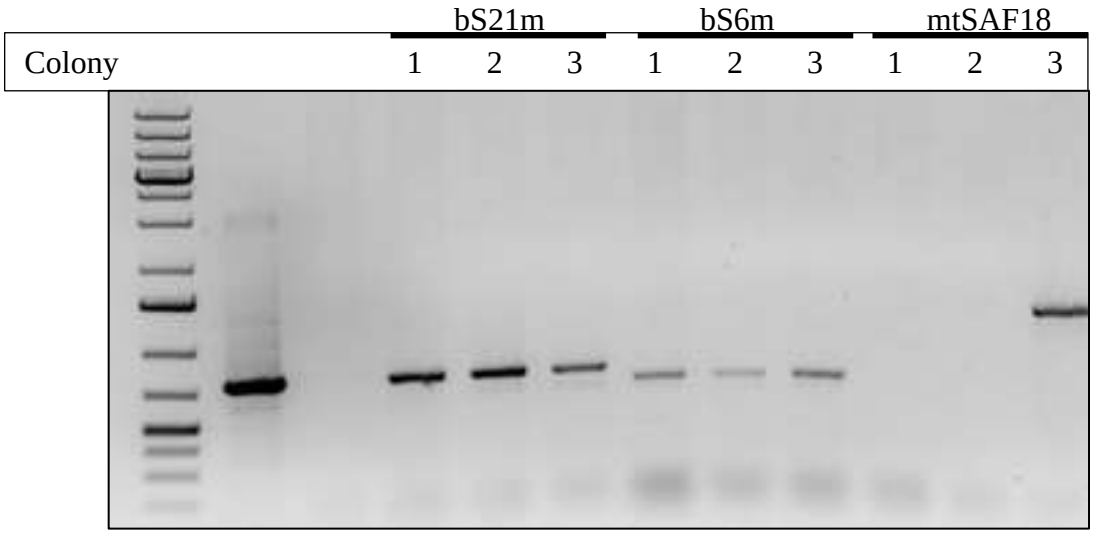

Figure 11: ***Agarose gel resolving results of PCR verification of the inserts****.*
The second and third lane contain positive (PC) and negative (NC) control, respectively.
The correct plasmids can be recognized by the bands at the corresponding sizes.

4.2 Purification of antigens for antibody production

From this step on, a fourth protein, mtSAF24 was included in the experiments. In the case of this protein, the plasmids were designed to only contain its N-terminal domain in order to be able to verify planned truncation of mtSAF24 in *T. brucei*. The cells containing plasmids coding for the antigen were prepared by a colleague.

First, an expression test was performed to select a suitable bacterial colony expressing the target protein for each of the four proteins. After testing of the recombinant proteins for their solubility, large-scale protein expression was performed. The proteins, containing the 6xHis tag, were purified with nickel column affinity chromatography and brought into the right conditions by dialysis and concentration assays. Finally, the proteins were submitted to David's Biotechnology for custom antibody production.

4.2.1 Expression and solubility test of recombinant proteins.

Two or three clones of *E. coli* containing expression plasmids for each recombinant protein were harvested before induction as well as three hours after induction with IPTG to determine whether they express mtSAF24, mtSAF18, bS6m or bS21m. In addition, in order to find a suitable affinity chromatography purification method, the solubility of the recombinant proteins was tested with Bug Buster reagent. SDS electrophoresis was performed to resolve the samples and to see if the expressed proteins ended up predominantly in the soluble or insoluble fraction.

bS6m (Figure 12) and mtSAF18 (Figure 13) were expressed in all tested clones. A large amount of the expressed proteins can be clearly recognized in the insoluble part of the lysates. For bS21m (Figure 14) only clone 1 seems to express the correct recombinant protein, which ended up as well in the pellet after solubilization.

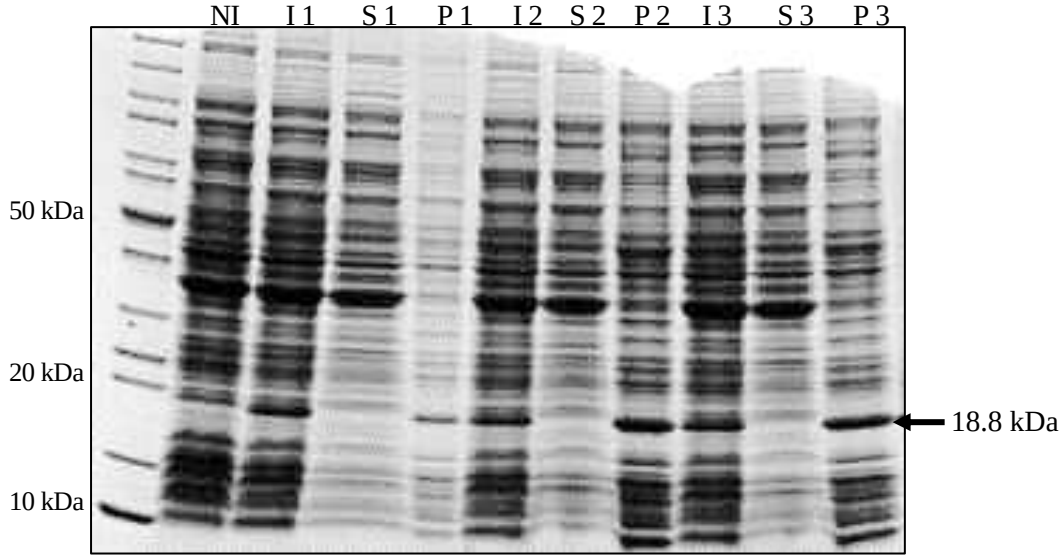

Figure 12: ***Expression and solubility test of three bS6m clones (1, 2, 3).***
Non-induced (NI), induced (I), soluble (S) and insoluble fraction (P) were resolved by SDS-PAGE and stained by Coomassie Blue.
The band corresponding to the protein is marked with arrow.

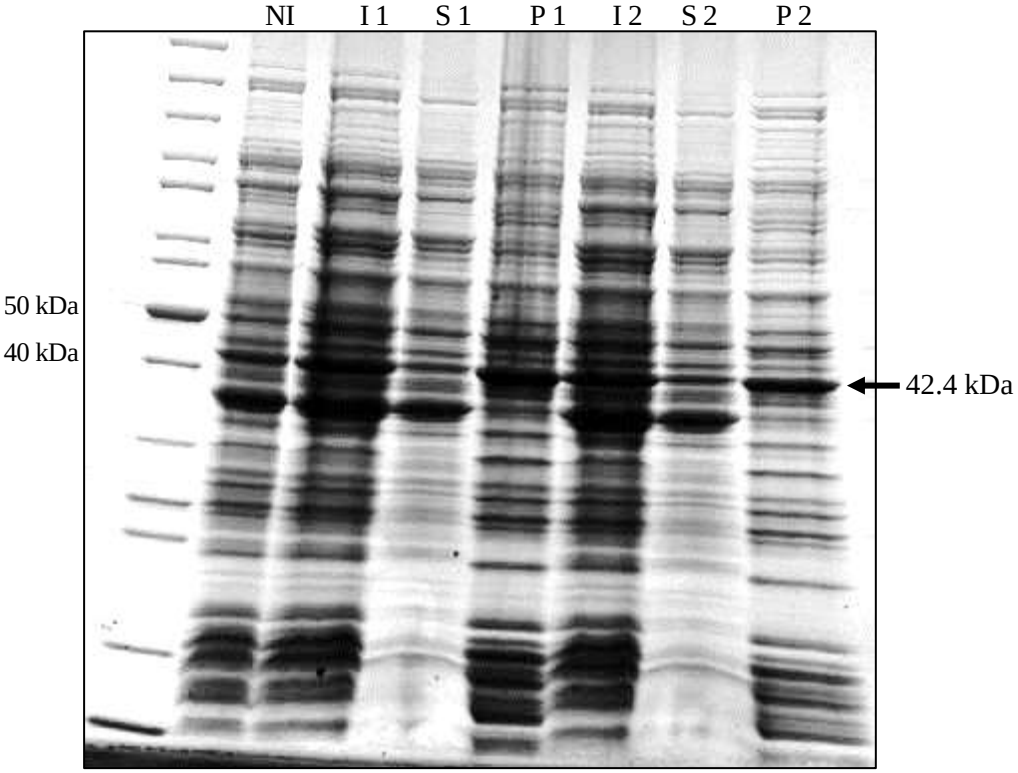

Figure 13: ***Expression and solubility test of two mtSAF18 clones (1, 2).***
Non-induced (NI), induced (I), soluble (S) and insoluble fraction (P) were resolved by SDS-PAGE and stained by Coomassie Blue.
The band corresponding to the protein is marked with arrow.

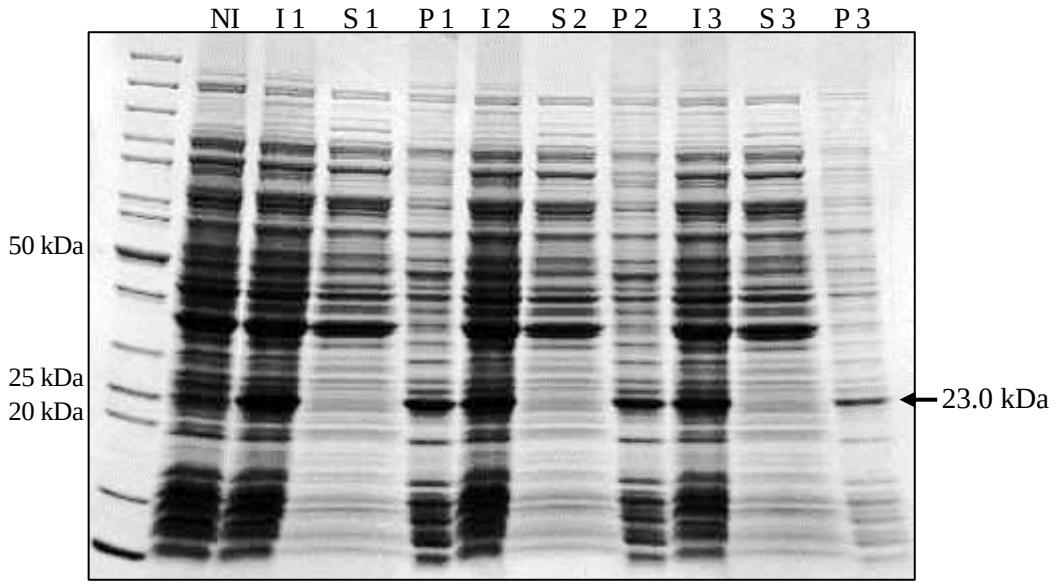

Figure 14: ***Expression and solubility test of three bS21m clones (1, 2, 3).***
Non-induced (NI), induced (I), soluble (S) and insoluble fraction (P) were resolved by SDS-PAGE and stained by Coomassie Blue.
The band corresponding to the protein is marked with arrow.

Also, the expression of the antigen containing the N-terminal domain of mtSAF24 was successful. The 12.2 kDa fragment can be seen in Figure 14. Solubility test revealed that the protein was likewise predominantly insoluble.

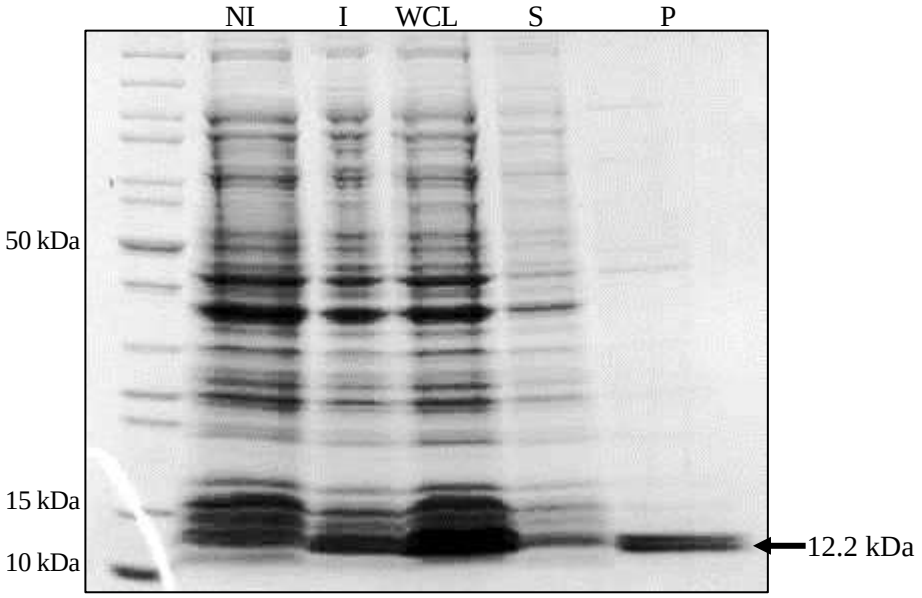

Figure 15: ***Expression and solubility test of clones containing N-terminal domain of mtSAF24.***
Non-induced (NI), induced (I), soluble (S) and insoluble fraction (P) were resolved by SDS-PAGE and stained by Coomassie Blue.
The band corresponding to the protein is marked with arrow.

Clones bS6m/2, mtSAF18/1 and bS21m/1 were chosen for large scale protein expression and purification.

4.2.2 Protein purification by affinity chromatography.

Recombinant proteins were purified by performing fast protein liquid chromatography (FPLC) with a Ni-NTA column on an ÄKTA Prime FPLC machine. Since all four proteins were determined to be insoluble, it was opted for a purification protocol containing sarkosyl to facilitate their solubilization. During the purification process the protein profile, produced by an UV detector, was monitored. The peaks seen in the UV profile were tested for presence of the respective recombinant protein. Hence samples were collected from each fraction starting one prior a peak in the UV profile until one fraction following the peak, additionally a sample from the flow-through was saved (40 µl sample + 20 µl SDS LD). The supernatants before sarkosyl solubilization were compared with the solubilized lysates, the unbound fractions (flow through), and with the fractions covering the peak. For bS21m and mtSAF18 insoluble fractions were not collected for SDS-PAGE and were therefore not included.

In Figure 16, the band corresponding to bS21m (23.0 kDa) can be clearly identified in the soluble fraction and as well in the insoluble one. This indicates that sarkosyl was not able to solubilize the protein entirely, therefore extensive part was lost. As expected, no protein was observed in the flow through, indicating that binding to the nickel column was successful. Almost all eluted protein was found in fractions F23 – F25, which corresponds to the second pronounced protein peak observed in the UV profile (Figure 17).

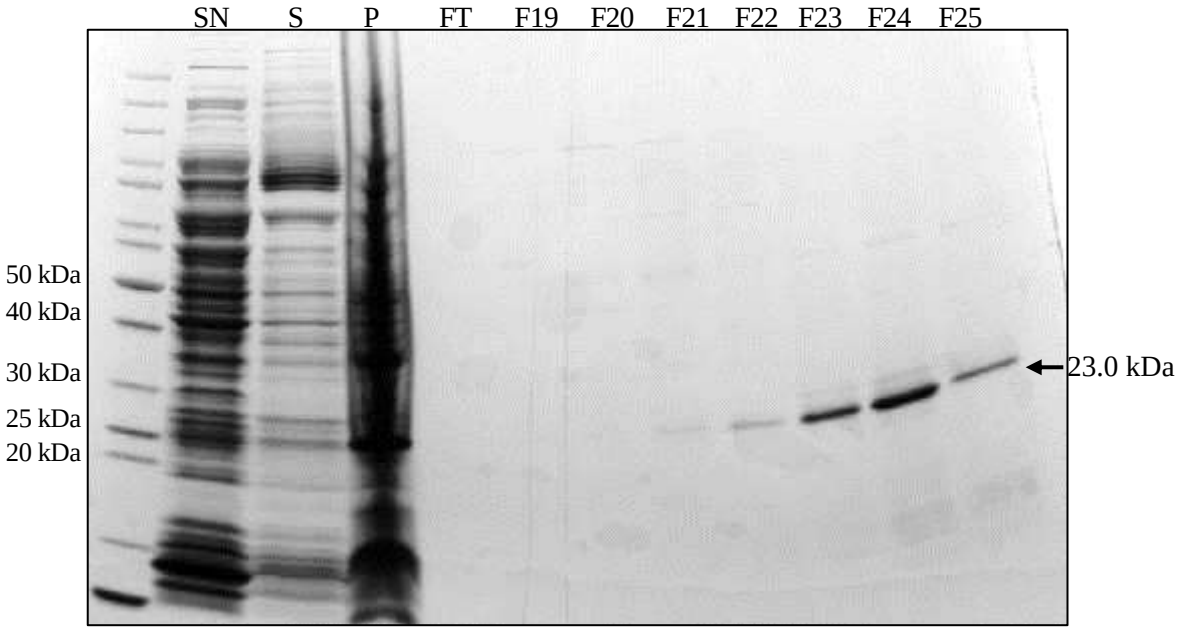

Figure 16: ***SDS-PAGE gel resolving purified proteins isolated from bS21m bacterial clone 1.***
30µl of samples and 5µl PageRuler Unstained Protein Ladder as size standard were loaded.
SN = supernatant prior solubilization; S = soluble parts; P = insoluble parts;
FT = flow through; F = purification fractions
Fraction numbers correlate with numbers depicted in the purification profile in Figure 17.
Fractions 23 – 25 were pooled for antibody production.

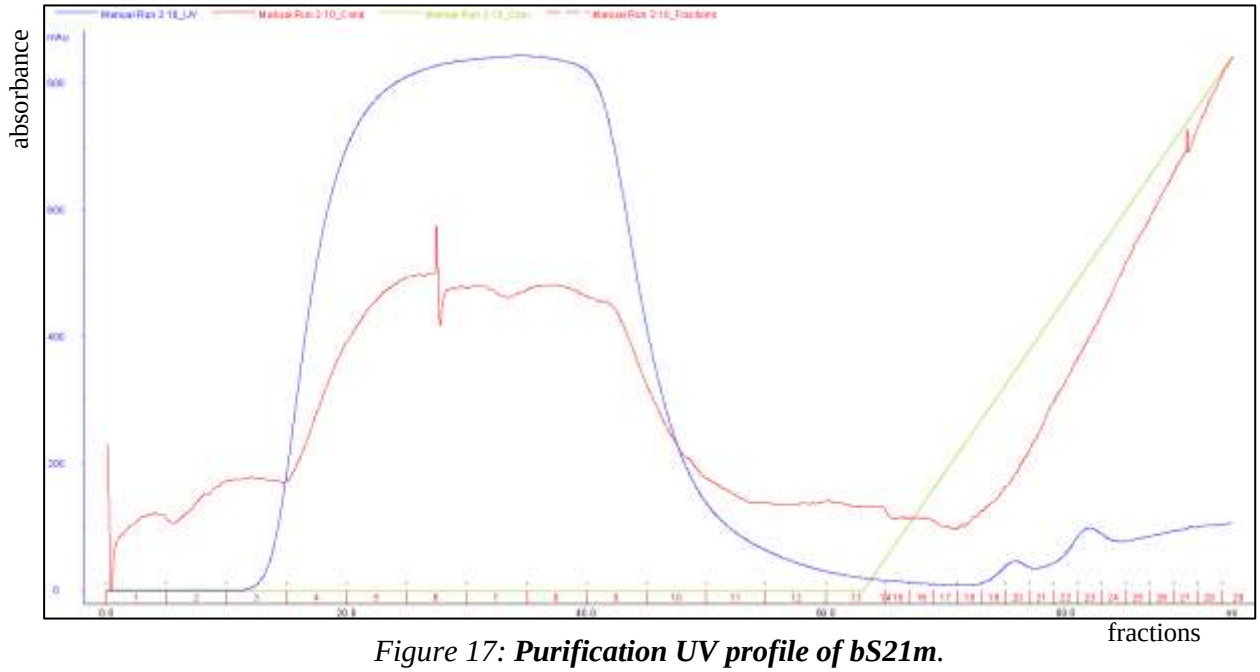

Figure 17: ***Purification UV profile of bS21m****.*
Green line indicates elution gradient. Protein peak begins at fraction 22.

The result for bS6m (18.8 kDa, Figure 18) was similar. A strong band was found in the soluble fraction, suggesting that the solubilization protocol did work. However, since the insoluble pellet was not kept, it was not known what proportion of protein remained insoluble. After elution, bS6m ended up predominantly in fractions F11 – F15, which agrees with the UV profile (Figure 19).

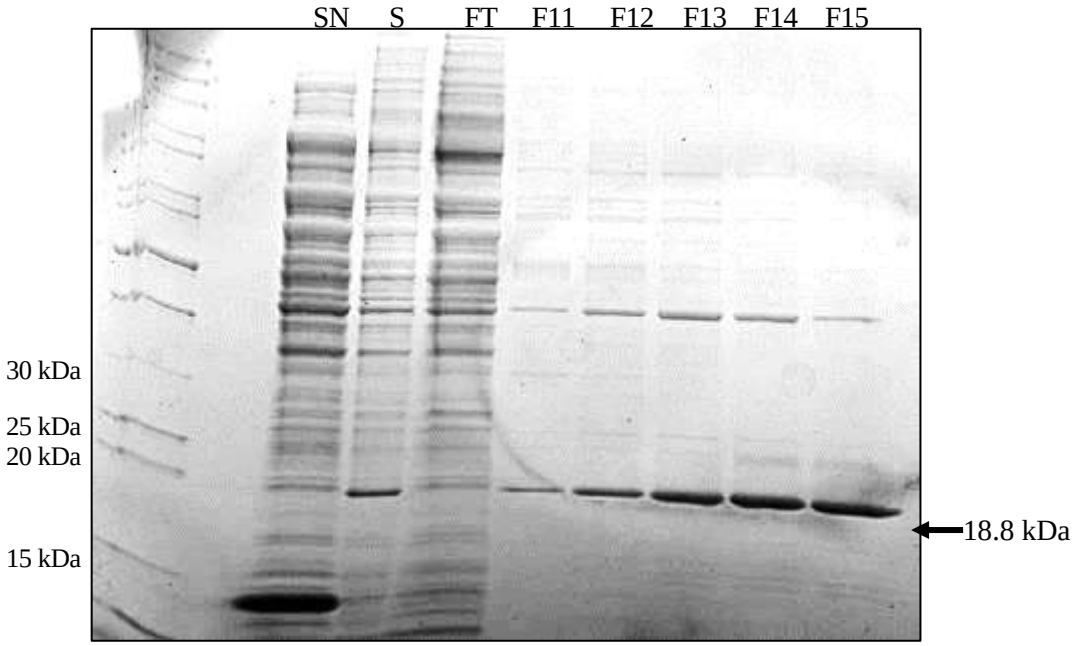

Figure 18: ***SDS-PAGE gel resolving purified proteins isolated from bS6m bacterial clone 2.***
30µl of samples and 5µl PageRuler Unstained Protein Ladder as size standard were loaded.
SN = supernatant prior solubilization; S = soluble parts; FT = flow through;
F = purification fractions
Fraction numbers correlate with numbers depicted in the purification profile in Figure 19.
Fractions 11 – 15 were pooled for antibody production.

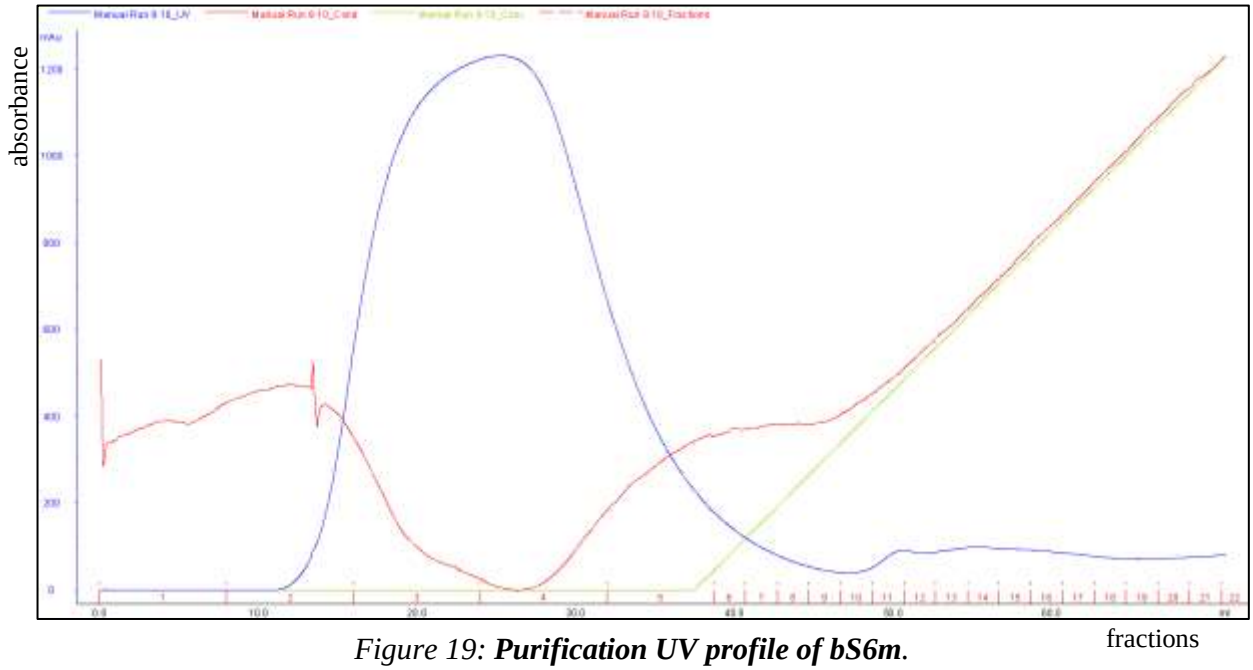

Figure 19: ***Purification UV profile of bS6m****.*
horizontal axis: fraction number; vertical axis: UV absorbance
Green line indicates elution gradient. Protein peak begins at fraction 11.

Although mtSAF18 (42.4 kDa, Figure 20) cannot be clearly identified in the soluble fraction after sarkosyl treatment, the purification did work. The recombinant protein was present in huge amount as thick bands in fractions F13 – F17 indicate. Especially for this protein, minor contaminations can be detected. The peak beginning at F13, indicating elution of protein, is also seen in the purification profile (Figure 21).

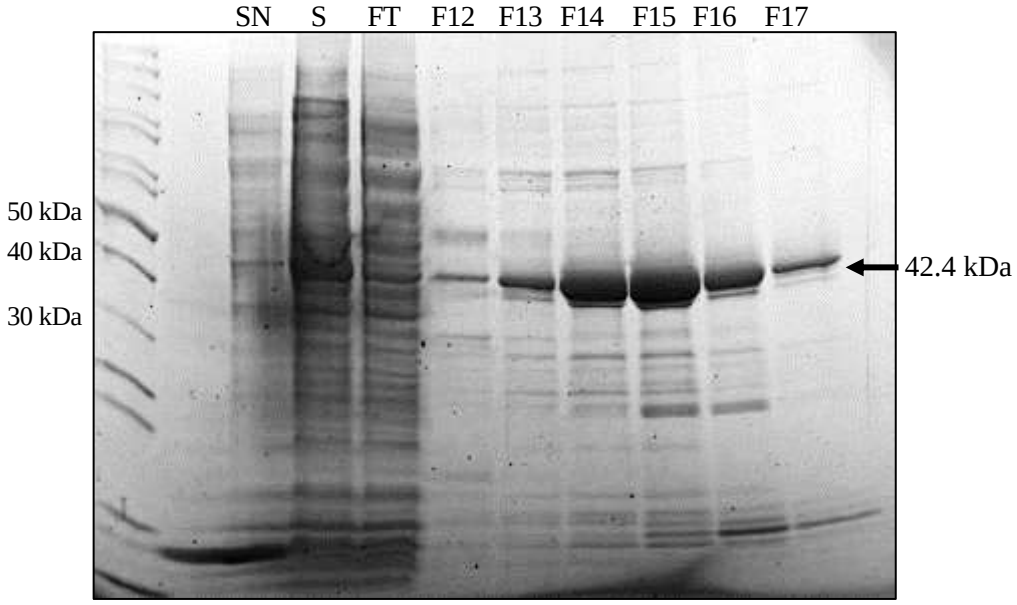

Figure 20: ***SDS-PAGE gel resolving purified proteins isolated from mtSAF18 bacterial clone 1.***
30µl of samples and 5µl PageRuler Unstained Protein Ladder as size standard were loaded.
SN = supernatant prior solubilization; S = soluble parts;
FT = flow through; F = purification fractions
Fraction numbers correlate with numbers depicted in the purification profile in Figure 21.
Fractions 13 – 17 were pooled for antibody production.

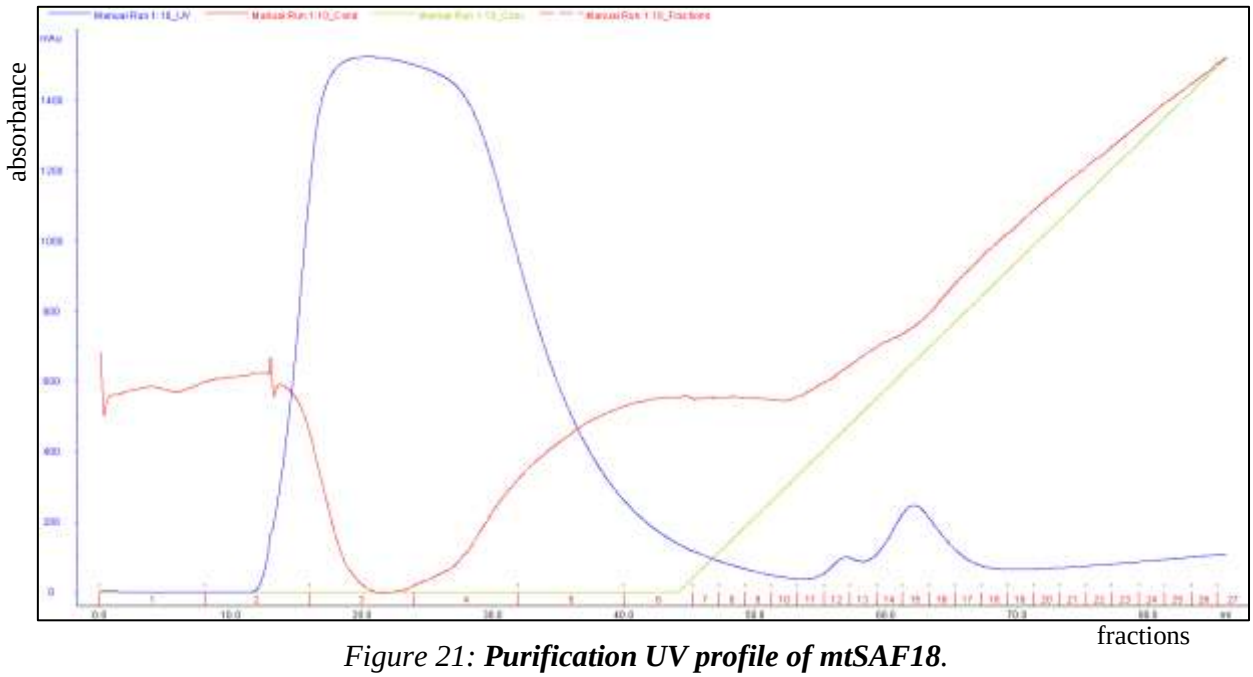

Figure 21: ***Purification UV profile of mtSAF18****.*
horizontal axis: fraction number; vertical axis: UV absorbance
Green line indicates elution gradient. Protein peak begins at fraction 13.

Although solubilization did as well only work partially (Figure 22), mtSAF24 (12.2 kDa) was present in huge amount in the obtained fractions. All screened fractions contained the protein in agreement with the peak in the UV profile (Figure 23).

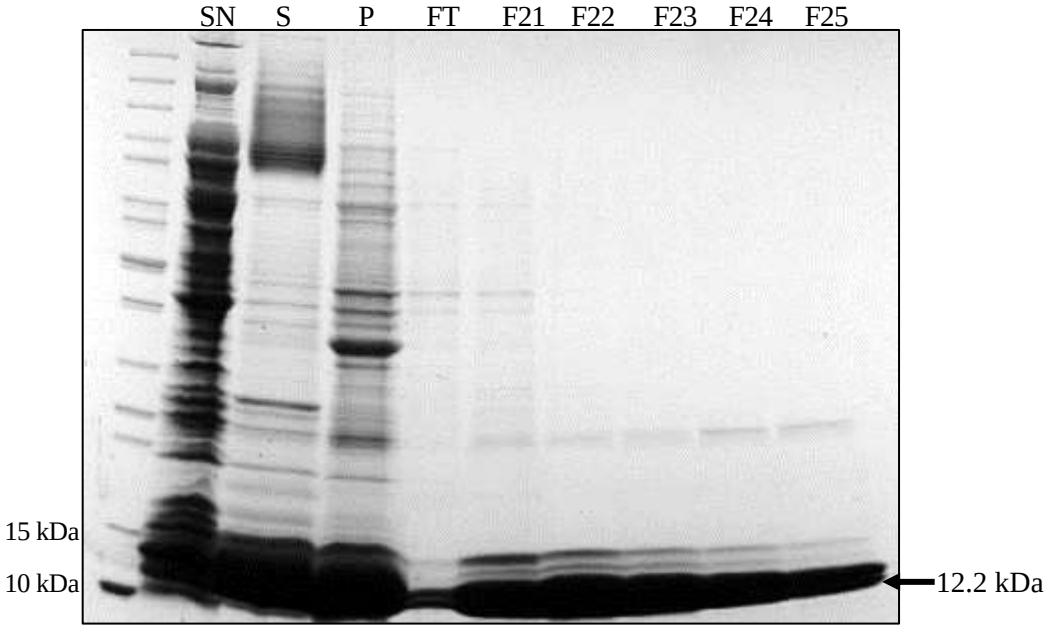

Figure 22: ***SDS-PAGE gel resolving purified proteins isolated from mtSAF24 bacterial clone.***
30µl of samples and 5µl PageRuler Unstained Protein Ladder as size standard were loaded.
SN = supernatant prior solubilization; S = soluble parts; P = insoluble parts;
FT = flow through; F = purification fractions
Fraction numbers correlate with numbers depicted in the purification profile in Figure 23.
Fractions 21 – 25 were pooled for antibody production.

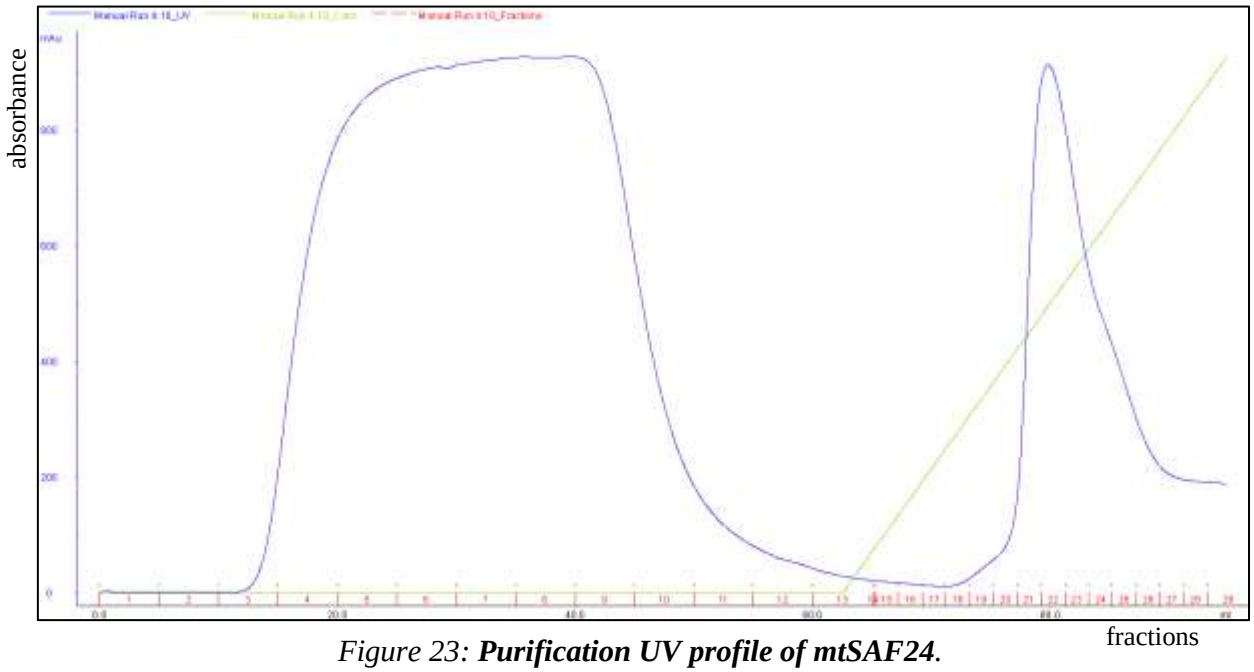

Figure 23: ***Purification UV profile of mtSAF24****.*
horizontal axis: fraction number; vertical axis: UV absorbance
Green line indicates elution gradient. Protein peak begins at fraction 21.

As the final aim was to submit the purified recombinant proteins as antigens to David's Biotechnology for production of antibodies, the concentration of sarkosyl was decreased to a concentration of 0.8 %. Fractions containing proteins were therefore pooled and dialyzed. Next concentration was determined to ensure that the protein yield was high enough for antibody production (Table 52).

Not all recombinant proteins initially fulfilled the requirements of a concentration between 0.3-2 mg/ ml, therefore further concentration steps had to be performed.

Table 52: Concentration of recombinant proteins after purification.

protein		**volume** [ml]	**concentration** [mg/ml]	**amount** [mg]
bS6m	before conc.	6	0.126	0.8
	after conc.	1.1	0.593	0.62
bS21m	before conc.	8	0.281	2.2
	after conc.	2	0.698	1.4
mtSAF18	before conc.	10	0.479	4.8
	after conc.	3.5	1.223	4.3
mtSAF24		10	2.100	21.0

Before shipping for antibody production, the quality of the proteins was verified again by SDS-PAGE as well as by a western blot with anti-6xHis-tag antibody (Figure 24).

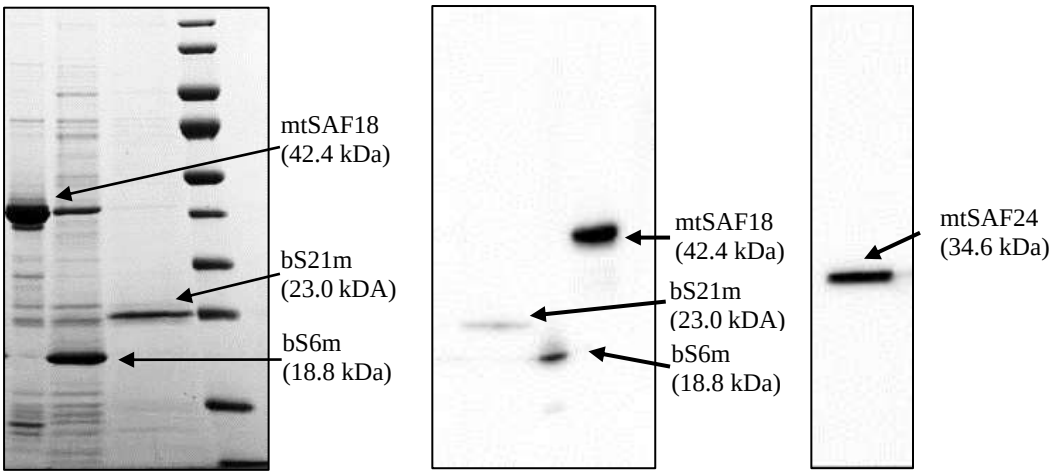

Figure 24: ***Purified proteins resolved on SDS-PAGE.***
left: Coomassie staining; right: Western-blot with anti-6xHis-tag antibody

David's Biotechnology makes use of roughly half of each protein as antigen for antibody production in the company's standard 63-day protocol, in which one rabbit was immunized with the respective antigen 5 times (0.5-1 mg of antigen in total). On day 35 a test bleed and enzyme-linked immunosorbent assay (ELISA) titer determination were performed to control the immunization process, followed, after the total interval of 63 days, by harvesting and affinity purification of the polyclonal antibodies from the antiserum using the second part of recombinant proteins (0.5 – 2 mg of each protein). Details on antibody production can be found here: https://www.davids-bio.com/pages/polyclonal-rabbit-antisera.html#polyclonal%20rabbit%20immunization.

4.3 Verification of antibodies

After receiving the polyclonal rabbit antibodies against either mtSAF18, mtSAF24, bS6m and bS21m from David's Biotechnology, the specificity of each was tested on organellar fraction, cytosolic lysate and WCL from procyclic form of *T. brucei* by western blotting. The lysates were prepared by fractionation using the mild detergent digitonin. Digitonin permeabilizes the cytoplasmic membrane, but the membrane of mitochondria and some other organelles, such as glycosomes (hence "organellar" fraction), remains intact.

Comprehensive testing was performed by repeating the experiment with different antibody concentrations, after several days of storage in different storing conditions (4°C, -20°C, and -20°C with added glycerol) and variations of probing times (1 hour, 2 hours or overnight) and temperatures (RT and 4°C). Only the best results are displayed in this section, further testing together with verification of submitochondrial localization of the target proteins was performed later in more advanced experiments (see section 8.4).

mtSAF24 (Figure 25)

The band at the expected size of 34.6 kDa was clearly detected in WCL and in organellar fraction. Additionally, the antibody bound to two proteins with a size of roughly 170 kDa, that are also present in the same two fractions.

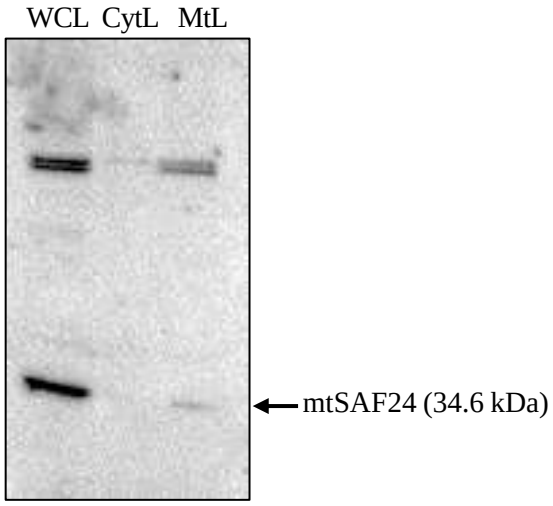

*Figure 25: Test of **anti-mtSAF24 antibody.***
Membranes probed with the antibody diluted 1:500 in PBS-T with 5% skimmed milk. Cytosolic fraction (CytL) and organellar fraction, containing mitochondria (MtL) from $1x10^7$ cells.

mtSAF18 (Figure 26)

Only very faint bands of the expected size were detected for the anti-mtSAF18 antibody in WCL as well as in the organellar fraction.

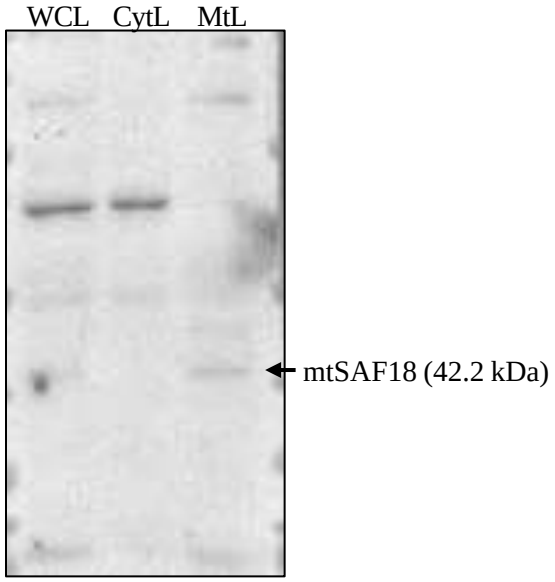

*Figure 26: Test of **anti-mtSAF18 antibody.***
Membranes probed with the antibody diluted 1:250 in PBS-T with 5% skimmed milk. Cytosolic fraction (CytL) and organellar fraction, containing mitochondria (MtL) from $1x10^7$ cells.

bS6m (Figure 27)

bS6m was neither detected in WCL or subcellular factions. However, the antibody clearly binds to the actual purified recombinant protein as well as to another protein, which might correspond to the prominent contamination of the recombinant bS6m observed on Coomassie stained gel (Figure 24).

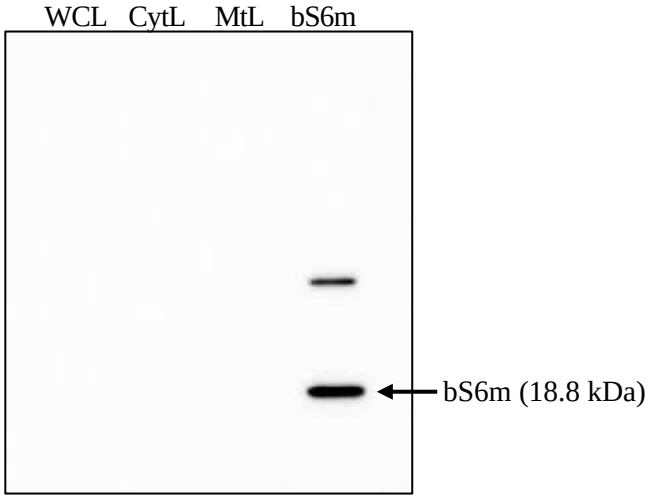

*Figure 27: Test of **anti-bS6m antibody.***
Membranes probed with the antibody diluted 1:250 in PBS-T with 5% skimmed milk. Cytosolic fraction (CytL) and organellar fraction, containing mitochondria (MtL) from $1x10^7$ cells. 9 µg of purified recombinant protein were loaded in the last lane.

bS21m

Upon repeated probing, the antibody against bS21m did not seem to recognize bS21m in any lysate. The expected band at 23.0 kDa was not recognized under short as well as long exposure.

4.4 Submitochondrial localization of mtSAF24, mtSAF18, bS6m and bS21m

To localize mtSAF24, mtSAF18, bS6m and bS21m in mitochondria of *T. brucei* cells, mitochondria purified by hypotonic lysis were fragmented by sonication and fractionated by centrifugation into mitochondrial matrix and mitochondrial membrane fraction. To distinguish between integral and peripheral membrane proteins, the membrane fraction was further split by Na_2CO_3 extraction.

Before probing with the generated antibodies, the purity of the collected fractions was determined by immunolabelling with different primary antibodies against proteins with well-established localization. For this reason, the samples collected from mitochondrial matrix,

mitochondrial membrane proteins, membrane peripheral proteins and integral membrane proteins were probed with antibodies against subunit β of mt F-ATP synthase (anti-β; membrane peripheral), AAC (membrane integral), Hsp70 (matrix) and SCoAS (matrix) overnight.

As shown in Figure 28, the transmembrane marker AAC, was only detected in the fraction containing membrane integral proteins, as expected. Anti-β recognizes a protein bound to mt membrane indirectly and should therefore be detected in fraction of peripheral proteins. However, some part of it was recognized in the mt matrix fraction, which might indicate that a part of loosely associated proteins was detached from the membrane by extensive sonication. Hsp70 was originally used as marker for the mt matrix, yet about half of the protein appears to be associated with the mt membrane. The dual Hsp70-localization is not surprising due to its multiple roles (Týč et al., 2015), among all in kDNA maintenance and folding of newly imported proteins (Craig, 2018). A slight Hsp70 signal seen in the integral membrane fraction indicated that Na_2CO_3 extraction was not able to split fractions completely. Because of the revealed association of Hsp70 with the mt membrane, the anti-SCoAS antibody was additionally employed as an alternative matrix marker. SCoAS is a soluble enzyme without functional link to mt membrane. Vast majority of SCoAS was detected in the matrix fraction, which proved the successful fractionation.

Since cross-contaminations of fractions were considered acceptable, the same samples were probed with mtSAF24, mtSAF18 and bS21m overnight.

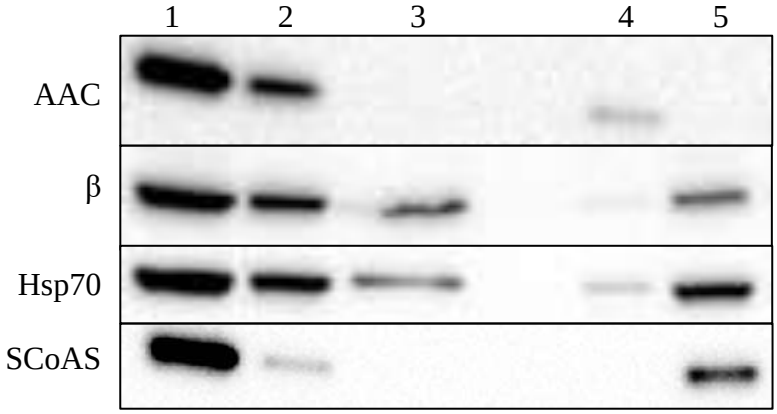

Figure 28: ***Western blot analysis to test efficiency of the subcellular fractionation.*** *Obtained fractions were probed with antibodies against the transmembrane marker AAC (53.5 kDa), the membrane peripheral β (71.5 kDA), Hsp70 (34 kDa), and the matrix marker SCoAS (44.9 kDa).*
1=mt; 2=mt membrane; 3=membrane associated; 4=membrane integral, 5=mt matrix

mtSAF24 (Figure 29)

The specific band for mtSAF24 at 34.6 kDa as well as the double-band at ~ 170 kDa were detected in the mt fraction. Additionally, another faint band appeared in mt fraction at roughly 60 kDa. A faint band in fraction 4 suggests that the ~170 kDa protein is embedded in the mt membrane. The concentration of Na_2CO_3 extracted samples was probably not sufficient for binding of the antibody.

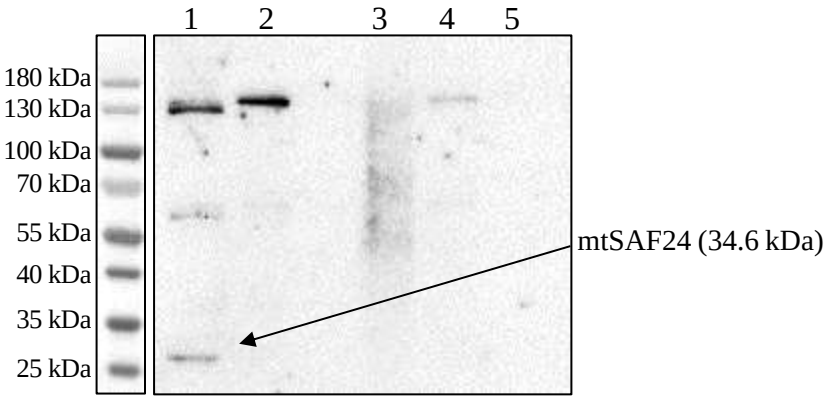

Figure 29: ***Localization testing of mtSAF24 on subcellular fractions.***
Fractions were probed overnight with anti-mtSAF24 diluted 1:500.
1=mt; 2=mt membrane; 3=membrane peripheral; 4=membrane integral, 5=mt matrix

mtSAF18 (Figure 30)

Although anti-mtSAF18 extensively bound non-specifically to various proteins, the target band at 42.2 kDa can be observed in mt lysate as well as in the membrane fraction. Additionally, a very weak band can be surmised in fraction 4, which would indicate that the protein is integrated into the membrane. The antibody behaved bizarrely in matrix fraction, which might have led to underrepresentation of the other lanes and probably hindered detection of further bands.

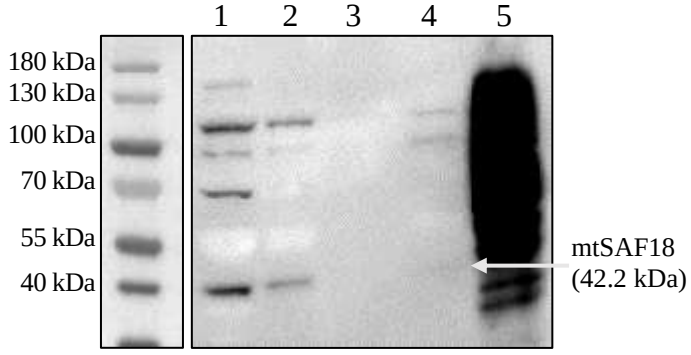

Figure 30: ***Localization testing of mtSAF18 on subcellular fractions****.*
Fractions were probed overnight with anti-mtSAF18 diluted 1:250.
1=mt; 2=mt membrane; 3=membrane peripheral; 4=membrane integral, 5=mt matrix

bS21m (Figure 31)

Similarly to the western blot of mtSAF18, the poor matrix fraction did not allow to interpret the results completely. The antibody bound to various non-specific bands. However, in mt fraction as well as mt membrane fraction it also recognized a roughly 23 kDa protein possibly corresponding to bS21m. Further fractions again were of too low concentration for bands to be detected.

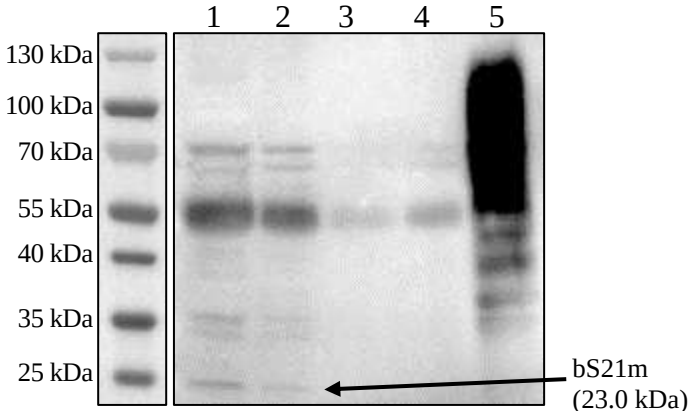

Figure 31: ***Localization testing of bS21m on subcellular fractions.***
Fractions were probed overnight with anti-bS21m diluted 1:250.
1=mt; 2=mt membrane; 3=membrane peripheral; 4=membrane integral, 5=mt matrix

4.5 Analysis of association of target proteins with mitoribosomal particles

This experiment aimed to verify the association of mtSAF24, mtSAF18 and bS6m with the mtSSU assembly intermediate, and bS21m's and bS6m's with the mature mtSSU, and test, whether these two complexes can be separated by differential centrifugation. For this purpose, WCL of *T. brucei* prepared by lysis with DDM were fractionated based on their sedimentation properties on a sucrose gradient. During the gradient formation, UV signal of the fractionator was monitored (Figure 32).

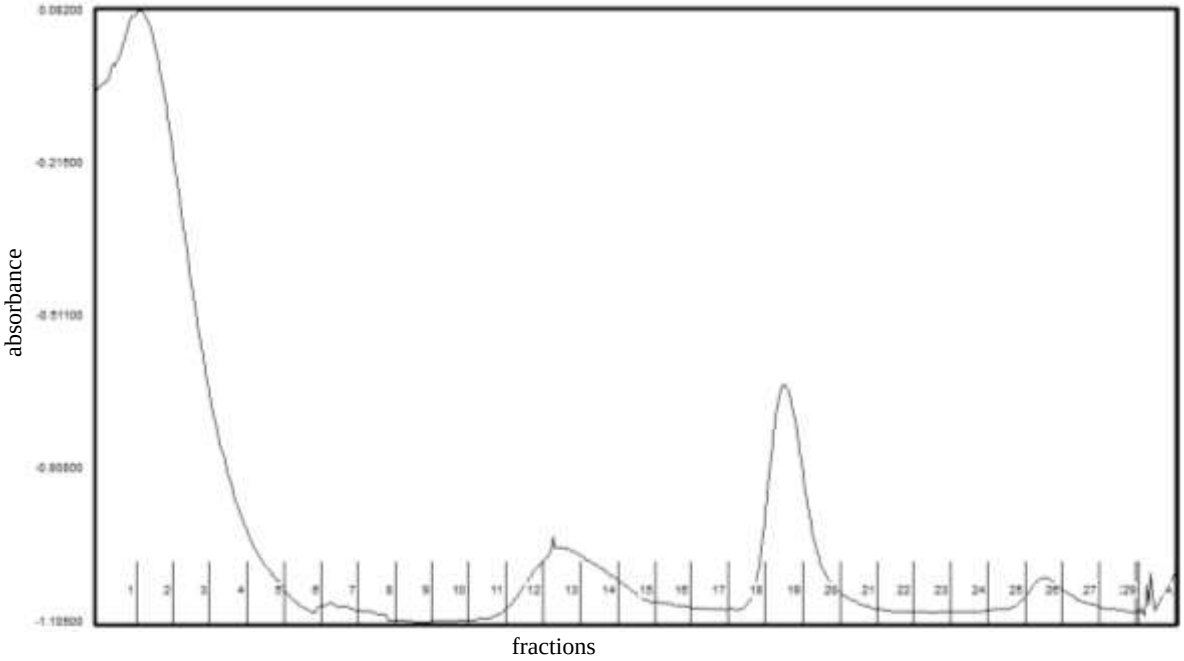

Figure 32: ***UV_{260nm} read out of the gradient station's Triax UV cell.***
vertical axis: absorbance; horizontal axis: fraction number

To determine the fractions containing mitoribosomal particles, RNA from the sedimentation fractions was isolated and then tested for presence of 12S (mtLSU), 9S (mtSSU) or 18S rRNA (cytoplasmic SSU) by dot blot and probing with ^{32}P-labeled oligos. Cytoplasmic 18S rRNA was included for confirming that the gradient fractionation worked. The dot blot (Figure 33) was quantified resulting in the most dominant signal in fraction 18 (Figure 34), which corresponds to the peak observed in the UV read out (Figure 32). Since cytoplasmic ribosomes are abundant, their presence in the peak was expected, and the UV peak can be used as a reference position for future experiments.

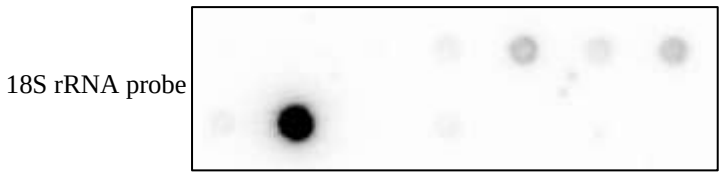

Fractions							
	2	4	6	8	10	12	14
	16	18	20	22	24	26	/

Figure 33: ***Dot blot of gradient sedimentation fractions hybridized with a ^{32}P-labeled 18S rRNA probe.***
Results were visualized by a Typhoon Phosphoimager. Table below indicates loaded fractions corresponding to numbering in Figure 32.

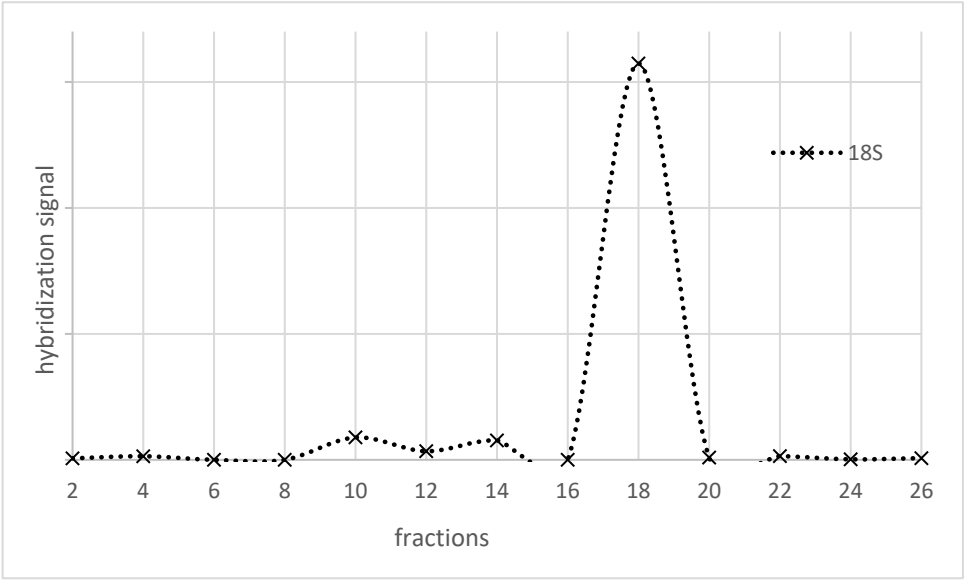

Figure 34: ***Sedimentation profiles of the 18 S rRNA.***
Ribonucleoprotein complexes contained in T. brucei WCL fractionated on sucrose gradient, RNA from fractions was extracted and hybridised on a dot blot with ^{32}P-labeled oligonucleotides. Signal in individual fractions was quantified and plotted. Fractions correspond to numbering in Figures 32 and 33.

Signal intensities seen in the dot blots (Figures 35) and seen after their quantification (Figure 36) suggest that the majority of 9S rRNA is present in fractions 8 – 14. 12S rRNA exhibits a major peak around fraction 10 and two minor peaks around fractions 2 and 16. Partial co-sedimentation of 9S rRNA with 12S RNA in the peak around fraction 10 indicates either the presence of the whole mitoribosomes in this part of the gradient or the fact, that mtSSU and mtLSU behave similarly during sedimentation.

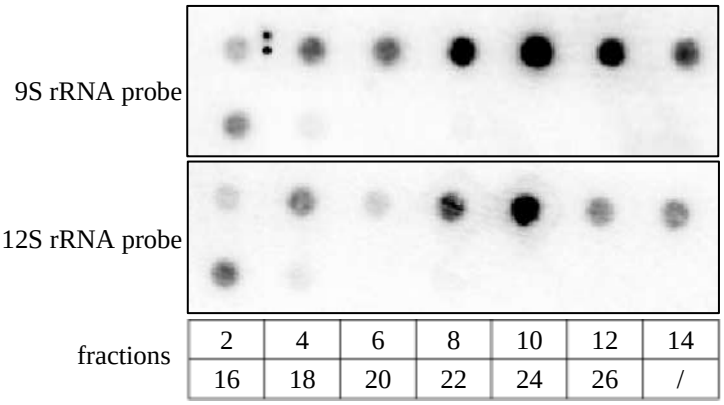

Figure 35: ***Dot blot of gradient sedimentation fractions hybridized with ^{32}P-labeled rRNA probes.***
Results were visualized by a Typhoon Phosphoimager. Table below indicates loaded fractions corresponding to numbering in Figure 33.

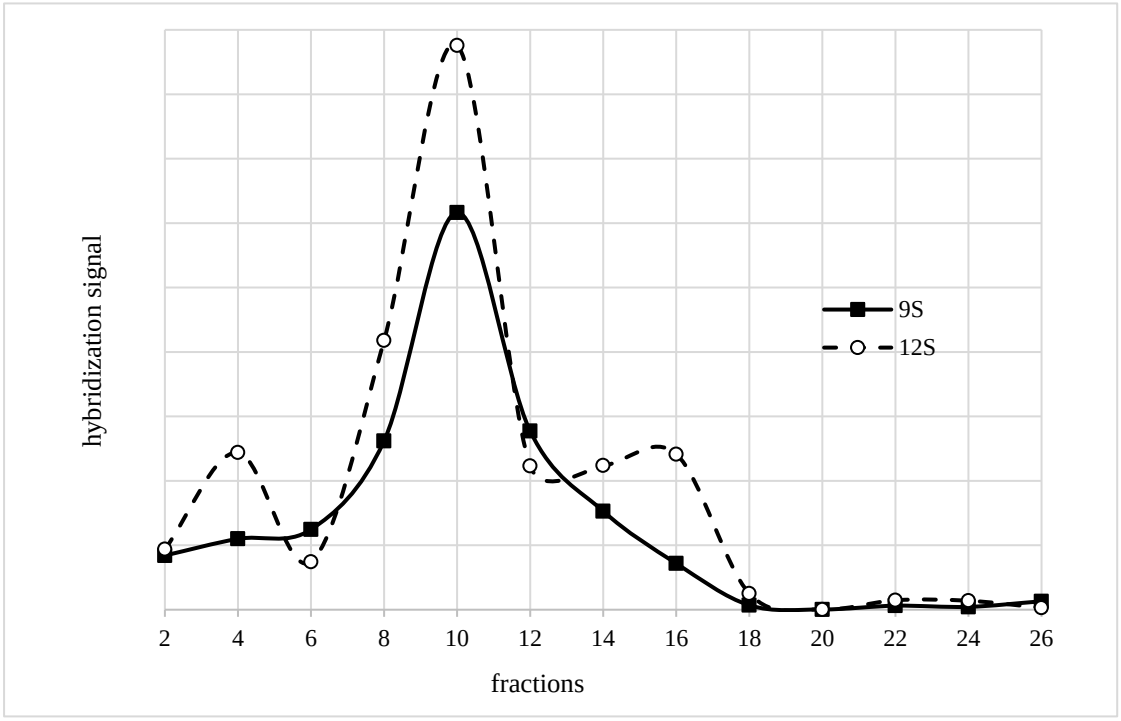

Figure 36: ***Sedimentation profiles of the 9 and 12 S rRNAs.***
Ribonucleoprotein complexes contained in T. brucei WCL fractionated on sucrose gradient, RNA from fractions was extracted and hybridised on a dot blot with ^{32}P-labeled oligonucleotides. Signal in individual fractions was quantified and plotted. Fractions correspond to numbering in Figures 32 and 35.

To determine the zones of the sucrose gradient that contain the mtSSU and the mtSSU assemblosome, fractions were subjected to immunoblotting with anti-mtSAF24, anti-mtSAF18, anti-bS21m or anti-bS6m. The fractions with signal from mtSAF18 and mtSAF24 would contain the mtSSU assemblosome, fractions with signal from bS21m contain the mature mtSSU, while bS6m should be detected in both complexes. The complexes can also partially or fully overlap in the gradient. However, due to an unpredictable technical issue, the results of western blotting were not informative. The experiment will be repeated with modifications (see Discussion).

5 Discussion

The function and biogenesis of the protein synthesis apparatus in mitochondria of *T. brucei* remains poorly understood. To increase knowledge related to the mitoribosome assembly pathway, recently received structural data of the mtSSU and the mtSSU assemblosome (Ramrath et al., 2018; Saurer et al., 2019) are further interpreted. In this project antibodies against two mtSSU components and two assembly factors were raised to track the mitoribosome and its precursor. In pilot experiments, antibodies were used to localize target proteins in *T. brucei* mitochondria and for determination of sucrose gradient fractions containing the mtSSU and the mtSSU assembly intermediate.

5.1 Antibody verification and detection of proteins in organellar fraction

Western blots showed that all the raised antibodies recognized the purified recombinant proteins. However, anti-bS6m did not bind to a protein of the expected size in any cell lysate. The polyclonal antibodies probably predominantly contain immunoglobulins recognizing some of the contaminations present in the purified recombinant bS6m, possibly due to a low antigenicity of the protein.

Anti-bS21m did not provide any meaningful results during the initial verification, yet, upon probing of the submitochondrial fractions, it detected a band of the expected size. However, due to the high non-specific signal, it cannot be reliable concluded that the band represents bS21m.

As expected, anti-mtSAF18 recognized the protein in WCL as well as in organellar fraction. Still, the signal was very low, and the antibody also produced various nonspecific bands. These obstructions might be explained also by contaminations in purified mtSAF18 or low antigenicity of the protein.

Anti-mtSAF24 repeatedly produced two bands. The lower band has the expected size of mtSAF24 (34.6 kDa). The upper band consistently seen at ~170 kDa might correspond to the pentamer of mtSAF24 in which it is present in the mtSSU assemblosome. It would indicate high stability of the pentamer and its resistance to the SDS treatment. Addition of other denaturing agents (TritonX or urea) to the sample did not help to denature the putative pentamer (data not shown). A possible method to determine the nature of the upper band would be the preparation of a mtSAF24 RNAi cell line. If, upon RNAi downregulation, both bands (34.6 kDa and 170 kDa) would be reduced, the pentamer theory would be confirmed. If only the 34.6 kDa band would be affected, the ~170 kDa band corresponds to another protein.

Furthermore, in contrast to depicted results (Figure 25) anti-mtSAF24 occasionally gave rise to the monomer's signal only in cytoplasmic fraction (Figure 39). An approach to verify the targeting of the protein in mitochondria would be immunostaining of fixed cells, followed by detection with fluorescent secondary antibodies and visualisation under fluorescent microscope (immunofluorescence assay, IFA). However, this assay might require better and more specific antibodies, than the ones raised during this project.

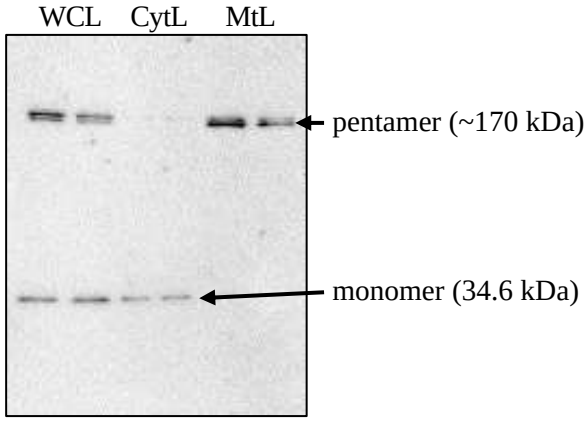

Figure 37: ***Western blot probed with mtSAF24 antibody.***
Membranes probed with the antibody diluted 1:500 in PBS-T with 5% skimmed milk. Cytosolic fraction (CytL) and organellar fraction, containing mitochondria (MtL) from $1x10^7$ cells.

Overall, quality of the produced antibodies is rather unsatisfactory. Yet they were used for further experiments, which produce samples of lower complexity and might therefore show lower extent of non-specific bands.

5.2 Submitochondrial fractionation

The protocol for submitochondrial fractionation by sonification followed by Na_2CO_3 extraction overall produced fractions in the expected quality. Although some mild cross-contaminations cannot be excluded (subunit β of mt F-ATP synthase was recognized in the matrix fraction), immunolabelling with control antibodies proved that the fractionation technique based on sonication in principle works. However, the weak signal of SCoAS in the membrane fraction indicates that the sonication was not able to lyse all mitochondria entirely. After the carbonate extraction, the residual unbroken mitochondria ended up in the membrane integral fraction, that is therefore apparently slightly contaminated by proteins enclosed in the intact mitochondria (beta, Hsp70). The purity might be improved by experimenting with varying parameters for sonication, or by clearing the sonicated material by short centrifugation prior the sedimentation of membrane pieces by ultracentrifugation.

The localisation test aimed to determine whether the mtSAFs are present either entirely in the matrix fraction or fully or partially in the membrane fraction, more specifically in the peripheral one. The former option would indicate that mtSSU assemblosome is not attached to inner mt membrane at all, while the latter would provide evidence for its membrane association.

Since bS21m is only recruited at a later stage of mitoribosome biogenesis, it is absent from the assemblosome. As free mature mtSSU is not expected to be connected to the mt membrane, whereas actively translating ribosomes are attached to it via mtLSU, the protein is expected to be detected in both fractions.

However, neither of these hypotheses could be confirmed or confuted with confidence since the antibodies behaved bizarrely in the matrix fraction and therefore the fraction could not be included for interpretation. Nevertheless, the obtained results suggest that both mtSAF18 and mtSAF24 are in the membrane fraction, confirming the assemblosomes' association with the membrane. Since in case of mtSAF24 only the ~170 kDa band was detected in the membrane fraction, the 34 kDa band might correspond to free monomeric mtSAF24, that is not yet incorporated into the assemblosome. Detection of the 34 kDa band in the matrix fraction would endorse this assumption. Thus, to interpret the data entirely, the experiment needs to be repeated.

5.3 Sedimentation analysis of mitoribosomal complexes

Observed sedimentation profiles of the sucrose gradient show extensive similarity with patterns previously observed in *T. brucei* (Ridlon et al., 2013, Figure 39). In the literature, co-sedimentation of 9S and 12S rRNA in fractions 19 – 21 indicate presence of complete ribosomes. The two overlapping peaks for 9S rRNA seen in fractions 13 – 17, most likely represent mature mtSSU and mtSSU assemblosome, since the latter one is slightly bigger as the mature complex. In contrast, the mtLSU shows similar size as its assembly complexes (Jaskolowski et al., 2020; Soufari et al., 2020; Tobiasson et al., in press), resulting in a total overlap of the peaks.

Since the gradient centrifugation was performed as a pilot experiment, the obtained profile does not resolve peaks in the same extent as previously (Ridlon et al., 2013). Only every second fraction was probed, which might have resulted in complete overlap of the mature mtSSU and mtSSU assemblosome peaks. Nonetheless, the experiment showed that fractionation of mitoribosomal complexes on sucrose gradient in general works. Consequently, the protocol can be used to repeat this experiment to achieve higher resolution by probing all fractions.

As already mentioned, immunoblotting with anti-mtSAF24, anti-mtSAF18, anti-bS21m or anti-bS6m will enable to determine the zones of the sucrose gradient that contain the mtSSU and the mtSSU assemblosome more precisely. However, because the experiment was designed and optimized for RNA analysis by dot blot probing, the individual fractions had too little concentration for immunolabelling. Using more cells as input material should circumvent this problem. Alternatively, the fractions might be concentrated by precipitation before performing western blots.

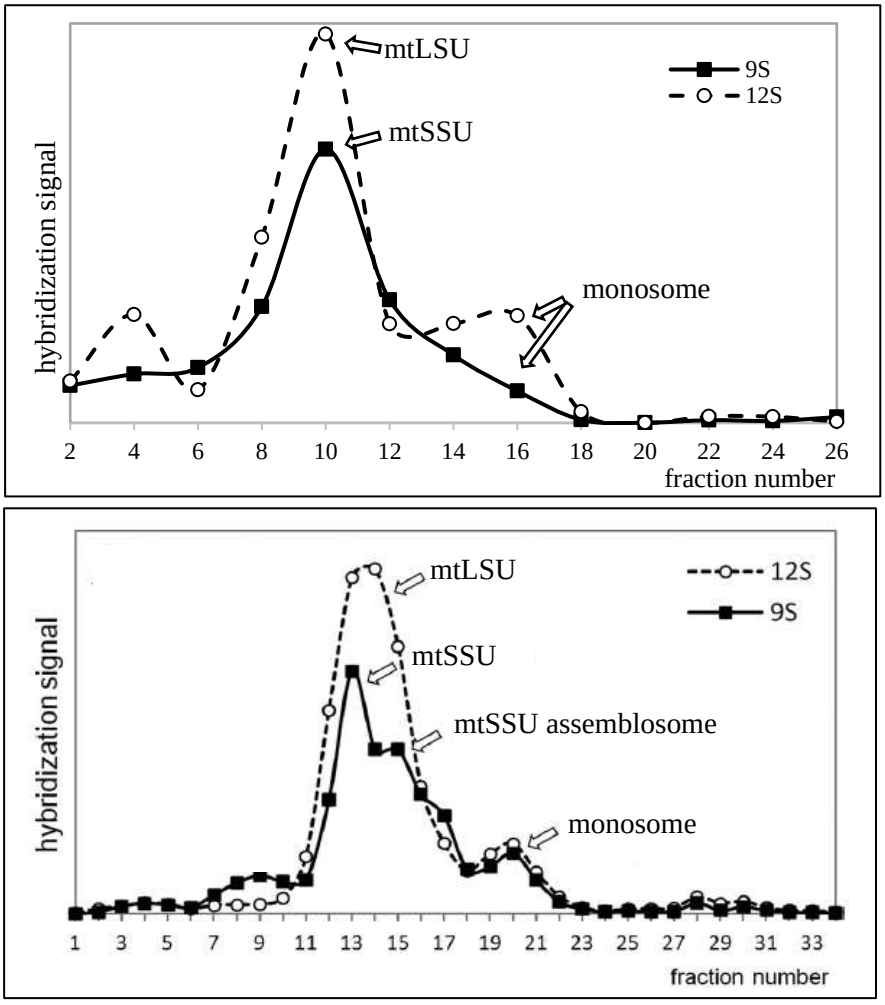

*Figure 38**: Comparison of sedimentation profiles of the 9 and 12 S rRNAs.***
Ribonucleoprotein complexes contained in T. brucei WCL fractionated on sucrose gradient, RNA from fractions was extracted and hybridised on a dot blot with ^{32}P-labeled oligonucleotides. Results were quantified and converted into a graph.
Lower image showing the profile observed by Ridlon et al., 2013 with changed labelling.

6 References

Barrell, B. G., Bankier, A. T., & Drouin, J. (1979). A different genetic code in human mitochondria. *Nature*, *282*(5735), 189–194. https://doi.org/10.1038/282189a0

Benne, R., De Vries, B. F., Van Den Burg, J., & Klaver, B. (1983). The nucleotide sequence of a segment of Trypanosoma brucei mitochondrial maxi-circle DNA that contains the gene for apocytochrome b and some unusual unassigned reading frames. *Nucleic Acids Research*, *11*(20), 6925–6941. https://doi.org/10.1093/nar/11.20.6925

Bieri, P., Greber, B. J., & Ban, N. (2018). High-resolution structures of mitochondrial ribosomes and their functional implications. *Curr Opin Struct Biol*, *49*, 44–53. https://doi.org/10.1016/j.sbi.2017.12.009

Braymer, J. J., & Lill, R. (2017). Iron-sulfur cluster biogenesis and trafficking in mitochondria. *The Journal of Biological Chemistry*, *292*(31), 12754–12763. https://doi.org/10.1074/jbc.R117.787101

Cavalier-Smith, T. (2006). Origin of mitochondria by intracellular enslavement of a photosynthetic purple bacterium. *Proceedings of the Royal Society B: Biological Sciences*, *273*(1596), 1943–1952. https://doi.org/10.1098/rspb.2006.3531

Craig, E. A. (2018). Hsp70 at the membrane: Driving protein translocation. In *BMC Biology* (Vol. 16, Issue 1). BioMed Central Ltd. https://doi.org/10.1186/s12915-017-0474-3

Daley, D. O., & Whelan, J. (2005). Why genes persist in organelle genomes. *Genome Biology*, *6*(5), 110. https://doi.org/10.1186/gb-2005-6-5-110

Davis, J. H., & Williamson, J. R. (2017). Structure and dynamics of bacterial ribosome biogenesis. *Philos Trans R Soc Lond B Biol Sci*, *372*(1716). https://doi.org/10.1098/rstb.2016.0181

De Silva, D., Tu, Y. T., Amunts, A., Fontanesi, F., & Barrientos, A. (2015). Mitochondrial ribosome assembly in health and disease. *Cell Cycle*, *14*(14), 2226–2250. https://doi.org/10.1080/15384101.2015.1053672

Eperon, I. C., Janssen, J. W., Hoeijmakers, J. H., & Borst, P. (1983). The major transcripts of the kinetoplast DNA of Trypanosoma brucei are very small ribosomal RNAs. *Nucleic Acids Research*, *11*(1), 105–125. https://doi.org/10.1093/nar/11.1.105

Etheridge, R. D., Aphasizheva, I., Gershon, P. D., & Aphasizhev, R. (2008). 3' adenylation determines mRNA abundance and monitors completion of RNA editing in T. brucei mitochondria. *EMBO J*, *27*(11), 1596–1608. https://doi.org/10.1038/emboj.2008.87

Feagin, J. E., Abraham, J. M., & Stuart, K. (1988). Extensive editing of the cytochrome c oxidase III transcript in Trypanosoma brucei. *Cell*, *53*(3), 413–422. https://doi.org/10.1016/0092-8674(88)90161-4

Grams, J., Morris, J. C., Drew, M. E., Wang, Z., Englund, P. T., & Hajduk, S. L. (2002). A trypanosome mitochondrial RNA polymerase is required for transcription and replication. *Journal of Biological Chemistry*, *277*(19), 16952–16959. https://doi.org/10.1074/jbc.M200662200

Hancock, K., & Hajduk, S. L. (1990). The mitochondrial tRNAs of Trypanosoma brucei are nuclear encoded. *J Biol Chem*, *265*(31), 19208–19215. https://www.ncbi.nlm.nih.gov/pubmed/2229071

Helm, M., Brulé, H., Friede, D., Giegé, R., Pütz, D., & Florentz, C. (2000). Search for characteristic structural features of mammalian mitochondrial tRNAs. *RNA (New York, N.Y.)*, *6*(10), 1356–1379. https://doi.org/10.1017/s1355838200001047

Jaskolowski, M., Ramrath, D. J. F., Bieri, P., Niemann, M., Mattei, S., Calderaro, S., Leibundgut, M., Horn, E. K., Boehringer, D., Schneider, A., & Ban, N. (2020). Structural Insights into the Mechanism of Mitoribosomal Large Subunit Biogenesis. *Mol Cell*. https://doi.org/10.1016/j.molcel.2020.06.030

Kehrein, K., Schilling, R., Möller-Hergt, B. V., Wurm, C. A., Jakobs, S., Lamkemeyer, T., Langer, T., & Ott, M. (2015). Organization of Mitochondrial Gene Expression in Two Distinct Ribosome-Containing Assemblies. *Cell Reports*, *10*(6), 843–853. https://doi.org/https://doi.org/10.1016/j.celrep.2015.01.012

Kennedy, P. G. (2013). Clinical features, diagnosis, and treatment of human African trypanosomiasis (sleeping sickness). *The Lancet. Neurology*, *12*(2), 186–194. https://doi.org/10.1016/S1474-4422(12)70296-X

Kennedy, P. G. E., & Rodgers, J. (2019). Clinical and Neuropathogenetic Aspects of Human African Trypanosomiasis . In *Frontiers in Immunology* (Vol. 10, p. 39). https://www.frontiersin.org/article/10.3389/fimmu.2019.00039

Koslowsky, D. J., & Yahampath, G. (1997). Mitochondrial mRNA 3' cleavage/polyadenylation and RNA editing in Trypanosoma brucei are independent events. *Molecular and Biochemical Parasitology*, *90*(1), 81–94. https://doi.org/10.1016/S0166-6851(97)00133-3

Kuzmenko, A. V, Levitskii, S. A., Vinogradova, E. N., Atkinson, G. C., Hauryliuk, V., Zenkin, N., & Kamenski, P. A. (2013). Protein biosynthesis in mitochondria. *Biochemistry (Moscow)*, *78*(8), 855–866. https://doi.org/10.1134/S0006297913080014

Leger, M. M., Petrů, M., Žárský, V., Eme, L., Vlček, Č., Harding, T., Lang, B. F., Eliáš, M., Doležal, P., & Roger, A. J. (2015). An ancestral bacterial division system is widespread in eukaryotic mitochondria. *Proceedings of the National Academy of Sciences*, *112*(33), 10239 LP – 10246. https://doi.org/10.1073/pnas.1421392112

Liu, B., Liu, Y., Motyka, S. A., Agbo, E. E., & Englund, P. T. (2005). Fellowship of the rings: the replication of kinetoplast DNA. *Trends Parasitol*, *21*(8), 363–369. https://doi.org/10.1016/j.pt.2005.06.008

Lukes, J., Hashimi, H., & Zikova, A. (2005). Unexplained complexity of the mitochondrial genome and transcriptome in kinetoplastid flagellates. *Curr Genet*, *48*(5), 277–299. https://doi.org/10.1007/s00294-005-0027-0

Maslov, D. A., Sharma, M. R., Butler, E., Falick, A. M., Gingery, M., Agrawal, R. K., Spremulli, L. L., & Simpson, L. (2006). Isolation and characterization of mitochondrial ribosomes and ribosomal subunits from Leishmania tarentolae. *Mol Biochem Parasitol*, *148*(1), 69–78. https://doi.org/10.1016/j.molbiopara.2006.02.021

McCutcheon, J. P., & Moran, N. A. (2012). Extreme genome reduction in symbiotic bacteria. *Nature Reviews Microbiology*, *10*(1), 13–26. https://doi.org/10.1038/nrmicro2670

Niemann, M., Schneider, A., & Cristodero, M. (2011). Mitochondrial translation in trypanosomatids: a novel target for chemotherapy? *Trends Parasitol*, *27*(10), 429–433. https://doi.org/10.1016/j.pt.2011.03.011

Petrov, A. S., Wood, E. C., Bernier, C. R., Norris, A. M., Brown, A., & Amunts, A. (2019). Structural Patching Fosters Divergence of Mitochondrial Ribosomes. *Mol Biol Evol*, *36*(2), 207–219. https://doi.org/10.1093/molbev/msy221

Pfeffer, S., Woellhaf, M. W., Herrmann, J. M., & Forster, F. (2015). Organization of the mitochondrial translation machinery studied in situ by cryoelectron tomography. *Nat Commun*, *6*, 6019. https://doi.org/10.1038/ncomms7019

Pollard, V. W., Rohrer, S. P., Michelotti, E. F., Hancock, K., & Hajduk, S. L. (1990). Organization of minicircle genes for guide RNAs in trypanosoma brucei. *Cell*, *63*(4), 783–790. https://doi.org/https://doi.org/10.1016/0092-8674(90)90144-4

Promega Corporation. (2018). pGEM(R)-T and pGEM(R)-T Easy Vector Systems Technical Manual. *Instructions for the Use of Products*, 1–29. https://www.promega.co.uk/~/media/files/resources/protocols/technical manuals/0/pgem-t and pgem-t easy vector systems protocol.pdf

Ramrath, D. J. F., Niemann, M., Leibundgut, M., Bieri, P., Prange, C., Horn, E. K., Leitner, A., Boehringer, D., Schneider, A., & Ban, N. (2018). Evolutionary shift toward protein-based architecture in trypanosomal

mitochondrial ribosomes. *Science*, *362*(6413). https://doi.org/10.1126/science.aau7735

Read, L. K., Lukes, J., & Hashimi, H. (2016). Trypanosome RNA editing: the complexity of getting U in and taking U out. *Wiley Interdiscip Rev RNA*, *7*(1), 33–51. https://doi.org/10.1002/wrna.1313

Ridlon, L., Skodova, I., Pan, S., Lukes, J., & Maslov, D. A. (2013). The importance of the 45 S ribosomal small subunit-related complex for mitochondrial translation in Trypanosoma brucei. *J Biol Chem*, *288*(46), 32963–32978. https://doi.org/10.1074/jbc.M113.501874

Roger, A. J., Munoz-Gomez, S. A., & Kamikawa, R. (2017). The Origin and Diversification of Mitochondria. *Curr Biol*, *27*(21), R1177–R1192. https://doi.org/10.1016/j.cub.2017.09.015

Saurer, M., Ramrath, D. J. F., Niemann, M., Calderaro, S., Prange, C., Mattei, S., Scaiola, A., Leitner, A., Bieri, P., Horn, E. K., Leibundgut, M., Boehringer, D., Schneider, A., & Ban, N. (2019). Mitoribosomal small subunit biogenesis in trypanosomes involves an extensive assembly machinery. *Science*, *365*(6458), 1144–1149. https://doi.org/10.1126/science.aaw5570

Scheinman, A., Aguinaldo, A.-M., Simpson, A. M., Peris, M., Shankweiler, G., Simpson, L., & Lake, J. A. (1993). Reconstitution of a Minimal Small Ribosomal Subunit. In *The Translational Apparatus* (pp. 719–726). Springer US. https://doi.org/10.1007/978-1-4615-2407-6_68

Sharma, M. R., Koc, E. C., Datta, P. P., Booth, T. M., Spremulli, L. L., & Agrawal, R. K. (2003). Structure of the mammalian mitochondrial ribosome reveals an expanded functional role for its component proteins. *Cell*, *115*(1), 97–108. https://doi.org/10.1016/s0092-8674(03)00762-1

Soufari, H., Waltz, F., Parrot, C., Durrieu-Gaillard, S., Bochler, A., Kuhn, L., Sissler, M., & Hashem, Y. (2020). Structure of the mature kinetoplastids mitoribosome and insights into its large subunit biogenesis. *Proceedings of the National Academy of Sciences of the United States of America*, *117*(47). https://doi.org/10.1073/pnas.2011301117

Thermo Fisher Scientific - AT. (n.d.). Retrieved November 6, 2020, from https://www.thermofisher.com/at/en/home.html

Týč, J., Klingbeil, M. M., & Lukeš, J. (2015). Mitochondrial heat shock protein machinery Hsp70/Hsp40 Is indispensable for proper mitochondrial DNA maintenance and replication. *MBio*, *6*(1). https://doi.org/10.1128/mBio.02425-14

Verner, Z., Basu, S., Benz, C., Dixit, S., Dobakova, E., Faktorova, D., Hashimi, H., Horakova, E., Huang, Z., Paris, Z., Pena-Diaz, P., Ridlon, L., Tyc, J., Wildridge, D., Zikova, A., & Lukes, J. (2015). Malleable mitochondrion of Trypanosoma brucei. *Int Rev Cell Mol Biol*, *315*, 73–151. https://doi.org/10.1016/bs.ircmb.2014.11.001

Waltz, F., & Giegé, P. (2019). Striking Diversity of Mitochondria-Specific Translation Processes across Eukaryotes. *Trends in Biochemical Sciences*. https://doi.org/10.1016/j.tibs.2019.10.004

Wiedemann, N., & Pfanner, N. (2017). Mitochondrial Machineries for Protein Import and Assembly. *Annual Review of Biochemistry*, *86*(1), 685–714. https://doi.org/10.1146/annurev-biochem-060815-014352

Yusupova, G. Z., Yusupov, M. M., Cate, J. H., & Noller, H. F. (2001). The path of messenger RNA through the ribosome. *Cell*, *106*(2), 233–241. https://doi.org/10.1016/s0092-8674(01)00435-4